3. Hotta O, Miyazaki M, Furuta T, et al. Tonsillectomy and steroid pulse therapy significantly impact on clinical remission in patients with IgA nephropathy. Am J Kidney Dis. 2001;38:736–43.
4. Matsuzaki K, Suzuki Y, Nakata J et al. Nationwide survey on current treatments for IgA nephropathy in Japan. Clin Exp Nephrol. 2013 (epub ahead of print). http://link.springer.com/content/pdf/10.1007%2Fs10157-013-0779-7. Accessed 22 March 2013.
5. Reich HN, Troyanov S, Scholey JW, et al. Remission of proteinuria improves prognosis in IgA nephropathy. J Am Soc Nephrol. 2007;18:3177–83.
6. Hwang HS, Kim BS, Shin YS, et al. Predictors for progression in immunoglobulin A nephropathy with significant proteinuria. Nephrology. 2010;15:236–41.
7. Tatematsu M, Yasuda Y, Morita Y, et al. Complete remission within 2 years predicts a good prognosis after methylprednisolone pulse therapy in patients with IgA nephropathy. Clin Exp Nephrol. 2012;16:883–91.
8. Imai E, Horio M, Yamagata K, et al. Slower decline of glomerular filtration rate in the Japanese general population: a longitudinal 10-year follow-up study. Hypertens Res. 2008;31:433–41.
9. Iseki K, Tokashiki K, Iseki C, et al. Proteinuria and the risk of developing end-stage renal disease. Kidney Int. 2003;63:1468–74.
10. Pozzi C, Andrulli S, Del Vecchio L, et al. Corticosteroid effectiveness in IgA nephropathy: long-term results of a randomized, controlled trial. J Am Soc Nephrol. 2004;15:157–63.
11. Li PK, Leung CB, Chow KM, et al. Hong Kong study using valsartan in IgA nephropathy (HKVIN): a double-blind, randomized, placebo-controlled study. Am J Kidney Dis. 2006;47:751–60.
12. Endo M. Epidemiology and prognosis of IgA nephropathy. Nihon Jinzo Gakkai Shi. 2008;50:442–7.
13. Goto M, Wakai K, Kawamura T, et al. A scoring system to predict renal outcome in IgA nephropathy: a nationwide 10-year prospective cohort study. Nephrol Dial Transpl. 2009;24:3068–74.
14. Szeto CC, Lai FM, To KF, et al. The natural history of immunoglobulin A nephropathy among patients with hematuria and minimal proteinuria. Am J Med. 2001;110:434–7.
15. Shen P, He L, Li Y, et al. Natural history and prognostic factors of IgA nephropathy presented with isolated microscopic hematuria in Chinese patients. Nephron Clin Pract. 2007;106(4):c157–61.
16. Scientific Committee, Japanese Society of Nephrology. Evidence-based practice guideline for the treatment of CKD. Tokyo: Tokyo Igakusya; 2009.
17. Commitee for Diagnostic Guidelines of Hematuria. Guidelines for diagnosis of hematuria. Nihon Jinzo Gakkai Shi. 2006;48(Suppl):1–34.
18. Committee of revision of clinical practice guidebook 2012 for diagnosis and treatment of CKD. Clinical practice guidebook for diagnosis and treatment of chronic kidney disease 2012. Tokyo: Tokyo Igakusha; 2012.
19. Japanese Society of Nephrology. Nephrotic syndrome diagnosis guidelines. Nihon Jinzo Gakkai Shi. 2011;53:78–122.

Nephrol Dial Transplant (2012) 27: 1090–1097
doi: 10.1093/ndt/gfr403
Advance Access publication 21 July 2011

Tonsillar TLR9 expression and efficacy of tonsillectomy with steroid pulse therapy in IgA nephropathy patients

Daisuke Sato[1], Yusuke Suzuki[1], Tatsuya Kano[1], Hitoshi Suzuki[1], Joe Matsuoka[2], Hidenori Yokoi[3], Satoshi Horikoshi[1], Katsuhisa Ikeda[3] and Yasuhiko Tomino[1]

[1]Division of Nephrology, Department of Internal Medicine, Juntendo University Faculty of Medicine, Tokyo, Japan, [2]Clinical Research Center, Juntendo University Faculty of Medicine, Tokyo, Japan and [3]Department of Otorhinolaryngology, Juntendo University Faculty of Medicine, Tokyo, Japan

Correspondence and offprint requests to: Yasuhiko Tomino; E-mail: yasu@juntendo.ac.jp

Abstract

Background. Patients with IgA nephropathy (IgAN) often show aggravation of renal injury with macroscopic hematuria after mucosal infections, especially tonsillitis. We previously demonstrated the important role of mucosal Toll-like receptor 9 (TLR9) activation in the pathogenesis of murine IgAN. Moreover, a single nucleotide polymorphism (SNP) in *TLR9* was significantly associated with pathological severity in human IgAN. In this study, we investigated correlations between tonsillar TLR9 messenger RNA expression, *TLR9* SNP genotypes and clinical outcomes following tonsillectomy with steroid pulse therapy (SPT) in IgAN patients.

Methods. Tonsillar TLR9 expression was examined in IgAN ($n = 49$) and control ($n = 15$) patients who had undergone tonsillectomy. The correlations between tonsillar TLR9 expression level, *TLR9* SNP genotypes and clinical outcomes after tonsillectomy with SPT were examined.

Results. High expression of tonsillar TLR9 was observed in ~23% of IgAN patients. These patients showed stronger and earlier remission of hematuria and proteinuria than those with low TLR9 expression. Patients with the TT genotype of *TLR9* SNP (rs352140) had more severe renal damage than those with other genotypes. Patients whose serum IgA level decreased more than average after tonsillectomy (large ΔIgA) showed higher cumulative remission rates of proteinuria than patients with a smaller decrease in these levels (small ΔIgA). CT/CC genotypes were more dominant and tonsillar TLR9 expressions significantly higher in large ΔIgA patients than in small ΔIgA patients.

Conclusion. In IgAN patients, expression levels of tonsillar TLR9 and *TLR9* SNP were well correlated with the efficacy of tonsillectomy with SPT.

Keywords: IgA nephropathy; SNP; tonsillectomy; TLR9

Introduction

IgA nephropathy (IgAN) is the most common form of glomerulonephritis globally, accounting for 25–50% of patients with primary glomerulonephritis [1]. Long-term follow-up studies have shown that up to 25–30% of patients progress to end-stage kidney disease within 20–25 years [2]. Although the pathogenesis of IgAN remains unclear, IgA or IgA immune complexes are assumed to be a causative factor. IgAN patients often show exacerbation of the disorder with macroscopic hematuria following upper respiratory tract infections such as tonsillitis and pharyngitis, indicating that local immune responses in these mucosal organs may be involved in the pathogenesis of IgAN. In fact, tonsillectomy is effective in improving long-term renal survival in IgAN patients [3]. A combination of tonsillectomy and high-dose methylprednisolone has been reported to have a great impact on clinical remission in IgAN patients [4–6], and tonsillectomy alone decreases serum IgA levels in these patients [7, 8]. Moreover, production of not only IgA-positive cells but also polymeric IgA is increased in tonsils of IgAN patients [9–11], suggesting that tonsils may be a major site of nephritogenic IgA production.

The Toll-like receptor (TLR) is a family of pathogen recognition molecules that discriminate pathogens from self and activate suitable defense mechanisms involving the Th1 immune response [12]. TLRs on antigen-presenting cells also initiate and modulate adaptive immunity during infection [13]. To date, 10 types of human TLRs have been identified [14]. We recently reported that nasal challenge with CpG oligodeoxynucleotide (CpG-ODN), a ligand of TLR9, aggravated renal injury with elevation of albuminuria, serum IgA level and mesangial IgA deposition in an IgAN-prone mouse model [15]. We also found that a single nucleotide polymorphism (SNP) in *TLR9* (TT genotype in rs352140) in IgAN patients was an important risk factor for disease progression [15], indicating involvement of TLR9 in the pathogenesis of human IgAN. These findings led us to speculate

that activation of TLR9 in the mucosa and tonsils by exogenous antigens may contribute to the pathogenesis of IgAN.

The therapeutic validity of tonsillectomy for IgAN remains controversial as its rationale is unclear. In addition, a large, randomized control trial of tonsillectomy with steroid pulse therapy (SPT) undertaken by the Special Study Group on Progressive Glomerular Disease, Ministry of Health, Labor and Welfare of Japan has not been completed. Therefore, it is important to investigate how tonsillar TLR9 expression and *TLR9* SNPs contribute to the outcome of this therapy in IgAN patients. These investigations may provide pathogenic insights and indications for this therapy.

Materials and methods

Patients and treatment protocol

Forty-nine patients with biopsy-proven IgAN (17 males) who had undergone tonsillectomy at the Department of Otorhinolaryngology of Juntendo University Faculty of Medicine were analyzed (Table 1). Fifteen patients with chronic tonsillitis ($n = 10$), obstructive sleep apnea syndrome ($n = 4$) and orpalmoplantar pustulosis ($n = 1$) were enrolled as controls.

Using the prognostic criteria for IgAN published by the joint committee of the Special Study Group on Progressive Glomerular Disease of the Ministry of Health and Welfare of Japan and the Japanese Society of Nephrology [16], the renal lesions were classified into four grades according to light microscopy findings of renal specimens based on the percentage of glomerular sclerosis, adhesion of glomerular tufts to Bowman's capsules and formation of crescents or tubulointerstitial lesions. The renal damage grades of the 49 study patients were as follows: Grade I (good prognosis, $n = 1$), II (relatively good prognosis, $n = 6$), III (relatively poor prognosis, $n = 18$) and IV (poor prognosis, $n = 14$). The pathological grades of 10 patients were unknown (missing information). At least 2 weeks after tonsillectomy, the patients received three courses of SPT (methylprednisolone 0.5 g/day for 3 days) at intervals of 2 months. During therapy, prednisolone at 0.5 mg/ideal body weight (kg) was also administered once every 2 days. Before and after treatment, the patients were evaluated for the following clinical outcomes: proteinuria (g/g·creatinine; g/g·Cr), hematuria (mean number of erythrocytes/high power field; HPF) and serum IgA level (mg/dL). Clinical remission of hematuria was defined as ≤5 erythrocytes/HPF during the observation period. Similarly, clinical remission of proteinuria was defined as ≤0.15 g/g·Cr.

Our hospital's Institutional Review Board approved this study, and all subjects gave prior informed consent.

Table 1. Patients' profile just before treatment

Age (years old)	31.9 ± 7.9
Male:female	14:35
Duration until tonsillectomy (years)	5.6 ± 6.3
Prognostic criteria for IgAN[a] (cases)	
Good prognosis Grade I	1
Relatively good prognosis Grade II	6
Relatively poor prognosis Grade III	18
Poor prognosis Grade IV	14
Unknown	10
Chemistries	
sCr (mg/dL)	0.76 ± 2.7
BUN (mg/dL)	12.9 ± 2.7
eGFR[b] (mL/min/1.73m^2)	86.5 ± 23.2
Proteinuria (g/g·Cr)	0.75 ± 0.8
Hematuria (RBC/HPF)	25.1 ± 9.0

[a]Patients are divided clinically into four groups at the time of renal biopsy according to clinical guidelines for IgAN in Japan, second version 16.
[b]Estimated glomerular filtration rate (eGFR) is calculated by the next formula; eGFR (mL/min./1.73m^2) = $194 \times Cr^{-1.094} \times Age^{-0.287}$ (male), $194 \times Cr^{-1.094} \times Age^{-0.287} \times 0.739$ (female) (Japanese Association of Chronic Kidney Disease Initiative, 2008).

Real-time reverse transcription polymerase chain reaction (PCR) analysis

Tonsil samples were snap frozen in liquid nitrogen immediately after resection and stored at −80°C before use. Total RNA was extracted using the RNeasy mini kit (QIAGEN, Hilden, Germany) according to the manufacturer's instructions. RNA quantity was assessed using the NanoDrop ND-1000 spectrophotometer (NanoDrop Products, Wilmington, DE). A 16-μL reaction mixture containing 1 μg of RNA, 4 μL of 2.5 mmol/L dNTP mixture (Takara Biochemicals, Ohtsu, Japan) and 2 μL of Random Decamers RETROscript (Ambion Inc., Austin, TX) in RNase-free water was inactivated by heating at 80°C for 3 min. The product was added to 2 μL of 10× polymerase chain reaction (PCR) buffer (Takara Bio Inc., Shiga, Japan), 1 μL of Protector RNase Inhibitor (Roche Diagnostics Corp., Mannheim, Germany) and 0.5 μL of M-MLV Reverse Transcriptase (Invitrogen Corp., Carlsbad, CA), followed by incubation at 42°C for 60 min. The complementary DNA (cDNA) product was used for real-time PCR. A 3-μL aliquot of diluted cDNA, 1.25 μL of each TaqMan Gene Expression Assay (Applied Biosystems, Carlsbad, CA) (Table 2), 12.5 μL of TaqMan Gene Expression Master Mix (Applied Biosystems) and 8.25 μL of cDNA-free double-distilled (dd) H_2O were then mixed to obtain a final reaction mixture of 25 μL according to the manufacturer's instructions. The mixture was denatured and amplified using the 7500 Real-Time PCR system (Applied Biosystems) under the following conditions: 15 s at 95°C and 60 s at 60°C for 40 cycles. Negative controls (cDNA-free dd H_2O) were included in each reaction. For quantification of the PCR product, the samples were standardized with the PCR product for glyceraldehyde-3-phosphate dehydrogenase (GAPDH). The results of TLR9 and related subjects' messenger RNA (mRNA) expressions were obtained by three repeated independent experiments.

Determination of TLR9 *genotype*

The SNP of *TLR9* (rs352140) was examined in the 44 enrolled patients as we have previously shown that this polymorphism is associated with prognosis based on histological severity in Japanese IgAN patients [15]. Genomic DNA was collected from blood samples using the DNA extraction kit GENOMIX® (Talent SRL, Trieste, Italy). The SNP probes used for genotyping were purchased from Applied Biosystems. PCR was performed using Applied Biosystems' 7500 Real-Time PCR system and TaqMan genotyping PCR Master Mix (Applied Biosystems). The PCR program was 50°C for 2 min, 95°C for 10 min and 40 cycles at 95°C for 15 s and at 60°C for 1 min.

Tonsillar cell preparation

Tonsil samples were obtained from the patients who had undergone tonsillectomy in our hospital. These tissue samples were immediately dissected into small pieces and incubated for 40 min at 37°C with 1 mg/mL collagenase IV (Worthington Biochemical Corporation, Lakewood, NJ). Subsequently, pan tonsillar cells were dissociated with a 100-μm cell strainer, followed by three washes to remove the collagenase. These cells were suspended in BAMBANKER® (Nippon Genetics, Tokyo, Japan), kept at −80°C overnight and after a cell count were stored at −196°C before use.

Fluorescence imaging

Approximately 1×10^6 pan tonsillar cells were stained to obtain fluorescence images. In brief, the cell surface staining was performed using Phycoerythrin (PE)-conjugated anti-human BDCA2 antibody (Miltenyi Biotech, Tokyo, Japan), followed by incubation with Fc receptor-blocking reagent (Miltenyi

Table 2. TaqMan® gene expression assay

Gene symbol	Gene name	Assay ID	Ref seq
TLR9	Toll-like receptor 9	Hs00370913_s1	NM_017442.2
IFN-α	Interferon alpha	Hs00256882_s1	NM_024013.1
IFN-γ	Interferon gamma	Hs99999014_m1	NM_138880.2
IL-12	Interleukin-12	Hs00233688_m1	NM_002187.2
GAPDH	Glyceraldehyde-3-phophate dehydrogenase	Hs02786624_g1	NM_002046.3

Biotech) or anti-human CD19 antibody (Beckman Coulter, Tokyo, Japan). Intracellular staining was performed using FITC-conjugated anti-human TLR9 antibody (Santa Cruz Biotechnology, Santa Cruz, CA), with IntraPrep (Beckman Coulter) being used for fixation and permeabilization of the examined cells. The images were taken using Biozero BZ-8100 (Keyence, Osaka, Japan) with BZ Viewer™ (Keyence).

Flow cytometric analyses

Approximately 1×10^6 pan tonsillar cells were stained for flow cytometry.

To confirm TLR9 expression in B cells, these cells were stained using PE-conjugated anti-human CD19 antibody (Beckman Coulter) or PE-conjugated isotype-matched mouse IgG1 (BD Bioscience, Flankline Lakes, NJ). Intracellular staining was performed using FITC-conjugated anti-human TLR9 antibody (Santa Cruz Biotechnology). IntraPrep (Beckman Coulter) was used for fixation and permeabilization of the examined cells, following FACScan analysis using CellQuest™ (Becton Dickinson Immunocytometer System, San Jose, CA). To confirm TLR9 expression in plasmacytoid dendritic cells (pDCs), the cells were analyzed using the Human Plasmacytoid Dendritic Cell/TLR9 Kit (IMGENEX, San Diego, CA) according to the manufacturer's instructions. To exclude B cells, T cells and macrophages, populations negative for FITC-conjugated mixed antibodies (anti-human CD3, CD14, CD16, CD19, CD20 and CD56 antibodies) and positive for PerCP Cy-5.5-conjugated anti-human HLA-DR were collected from tonsillar cells. Alexa-Fluor 647-conjugated anti-human CD123 antibody was used for further purification of the pDC population. These cells were permeablilized and stained using the PE-conjugated anti-human TLR9 antibody and analyzed by flow cytometry with CellQuest™ (Becton Dickinson Immunocytometer System).

Statistical analysis

Data are expressed as mean ± SD. Differences between the groups were examined for statistical significance using Student's *t*-test. A P-value of 0.05 was considered statistically significant. Using the Fisher's exact test, we compared CT/CC and TT genotype patients results session.

Results

Patients with high TLR9 expression in tonsils showed good therapeutic outcomes

The mean values of tonsillar TLR9/GAPDH expression of the IgAN patients and controls were 4.75 ± 2.83 and 4.45 ± 2.26, respectively. Relatively high expression of TLR9 (>mean + SD) in tonsils was observed only in 11 of 49 IgAN patients (22.4%). The mean values were calculated for the IgAN and control samples. These 11 patients were designated as the high TLR9 group and the remaining IgAN patients as the low TLR9 group (Figure 1a).

Cumulative remission rates of hematuria and proteinuria in the high TLR9 group were higher than those in the low TLR9 group. However, statistically significant differences were observed in the remission rate of proteinuria between the high TLR9 and low groups before the second SPT ($P = 0.925$), before the third SPT ($P = 0.196$) or after the therapy ($P = 0.371$). In addition, no statistically significant differences were observed between these two groups in remission rate of hematuria before the second SPT ($P = 0.596$), before the third SPT ($P = 0.343$) or after the therapy ($P = 0.632$). Despite similar clinical backgrounds just before tonsillectomy (Table 3), clinical remission of proteinuria and hematuria appeared earlier in the TLR9 high-group than in the low TLR9 group (Figure 1b). In addition, the TLR9 expression level did not correlate significantly with duration from estimated onset to tonsillectomy, age or

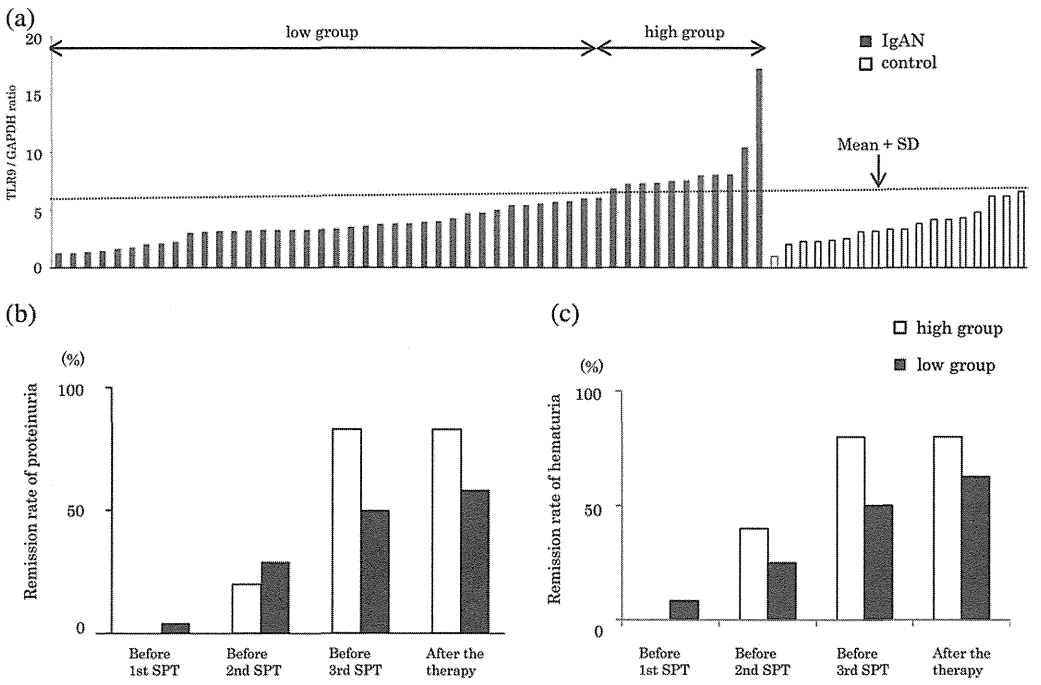

Fig. 1. (**a**) mRNA expression of TLR9. Total RNAs isolated from tonsillar tissues of IgAN patients and controls were reverse transcribed, and the mRNA levels of TLR9 determined by real-time PCR. Each sample dataset was standardized with mRNA expression of GAPDH. Of the 49 patients, 11 showed marked expression of TLR9 (>mean + SD). We defined these 11 patients as the high TLR9 group and the other patients as the low TLR9 group. We obtained the average value and SD from the IgA nephropathy patients and controls. The broken line represents the average + SD. (**b**, **c**) Comparison of cumulative remission rates of hematuria and proteinuria between the high TLR9 group and low group. In the high TLR9 group, designated by the open bar, the cumulative remission rates of hematuria and proteinuria were higher than those in the low TLR9 group. This response occurred at an earlier phase of this therapy than in the low TLR9 group, designated by the filled bar.

levels of proteinuria and hematuria at tonsillectomy (data not shown).

Patients with TT genotype TLR9 SNP *(rs352140) showed severe pathological damage and poor therapeutic outcomes*

We divided the patients into two groups according to their *TLR9* SNP (rs352140) genotype, TT or CT/CC, and then evaluated the clinical features and treatment responses in the two groups. The frequency of the TT genotype was ~23% in the 44 IgAN patients. No patient with a TT genotype was classified as Grades I/II (Grades I + II/III + IV: 0/9 in TT, 7/23 in CT/CC) (Table 4), suggesting that patients with this genotype tend to have more severe histological damage. In addition, expression of inflammatory cytokines such as IFN-α, IFN-γ and IL-12 in tonsils of TT genotype patients was higher than those in tonsils of CT/CC genotype patients (Table 4). Moreover, the remission rates of hematuria and proteinuria in TT genotype patients were lower than in CT/CC genotype patients (Table 4). At the last observation point, both TT and CT/CC genotype patients showed almost equal remission rates in urinary findings. We analyzed the correlation between TLR9 expression and *TLR9* SNP and showed that there was no significant difference in the tonsillar TLR9/GAPDH expression ratio [(CT/CC (n = 30) versus TT genotypes (n = 10); 2.86 ± 1.17 versus 2.45 ± 1.41; P = 0.64)]. In addition, the Fisher's exact test did not show a significant correlation between *TLR9* SNP (CT/CC and TT groups) and the expression level (TLR9 high-group and low-group) (P = 0.232).

Table 3. Clinical data of TLR9 high- and low-groups

	TLR9 high-group (N = 11)	TLR9 low-group (N = 38)
Duration until tonsillectomy (years)	5.9 ± 4.5	6.1 ± 7.2
sCr (mg/dL)	0.8 ± 0.2	0.7 ± 0.2
BUN (mg/dL)	12.4 ± 2.2	13.0 ± 2.8
eGFR (mL/min/1.73m^2)	79.0 ± 22.0	88.6 ± 23.4
Serum IgA (mg/dL)	338.5 ± 116.9	296.4 ± 98.2
Proteinuria (g/g·Cr)	0.9 ± 0.4	0.7 ± 0.7
Hematuria (RBC/HPF)	12.0 ± 0.1	26.3 ± 7.6

Patients whose serum IgA decreased more than the average by tonsillectomy alone had good therapeutic outcomes

To elucidate the relationship between the decrease in serum IgA level after tonsillectomy and treatment response, IgAN patients were divided into two groups according to their reduction in serum IgA levels. Both serum IgA levels before and after therapy could be evaluated in 30 patients. The levels decreased from 308.4 ± 103.0 to 279.2 ± 97.0 mg/dL, with the mean reduction rate in serum IgA being ~8.1%. The large ΔIgA group included patients whose serum IgA decreased more than the average (8.1%) following tonsillectomy alone, with the remaining 16 patients being designated as the small ΔIgA group. Patients in the large ΔIgA group showed higher cumulative remission rates of proteinuria and hematuria than those in the small ΔIgA group (Figure 2a and b). The expression levels of TLR9 mRNA in tonsils of the large ΔIgA group were significantly higher than those in the small ΔIgA group (P < 0.05) (Figure 2c). In addition, the percentage of TT genotype patients was obviously small in the large ΔIgA group (Table 5).

TLR9 expression in B cells or plasmacytoid dendritic cells

Figure 3a shows that parts of CD19$^+$ B cells or BDCA2$^+$ pDCs from tonsils of IgAN patients expressed TLR9. To further confirm these results, we examined the flow cytometric analyses. Figure 3b shows certain parts of CD19$^+$ B cells expressed TLR9 (FL-1; TLR9, FL2; CD19). Lineage negative (anti-human CD3, CD14, CD16, CD19, CD20 and CD56 antibodies) and HLA-DR-positive cells were gated as R1 for detection of DC (Figure 3c). Nextly, we

Table 4. Patient profiles, TLR9 and related cytokine expressions in tonsil and therapeutic efficacy of TT and CT/CC patients

Patients profiles	TT	CT/CC
Number	10	34
Gender (% female)	70.0	75.0
Duration until tonsillectomy (years)	3.5 ± 3.8	6.2 ± 7.1
Histopathological prognostic criteria (Grades I + II versus Grades III + IV)	0 versus 9	7 versus 24
Proteinuria before tonsillectomy (g/g·Cr)	1.1 ± 1.1	0.6 ± 0.5
Hematuria before tonsillectomy (RBC/HPF)	27.1 ±8.4	24.5 ± 9.2
Tonsillar expression of TLR9 and related cytokines		
TLR9	2.4 ± 1.3	3.0 ± 1.4
IFN-α	36.0 ± 58.8	30.2 ± 54.6
IFN-γ	7.3 ± 3.3	5.6 ± 4.8
IL-12	22.5 ± 21.0	12.2 ± 12.9
Therapeutic efficacy		
Remission rate after first SPT (%)		
Hematuria	12.5 (1/8)	31.8 (7/22)
Proteinuria	37.5 (3/8)	52.6 (10/19)
Remission rate 1 year after the start of treatment (%)		
Hematuria	62.5 (5/8)	63.6 (14/22)
Proteinuria	75.0 (6/8)	78.9 (15/19)

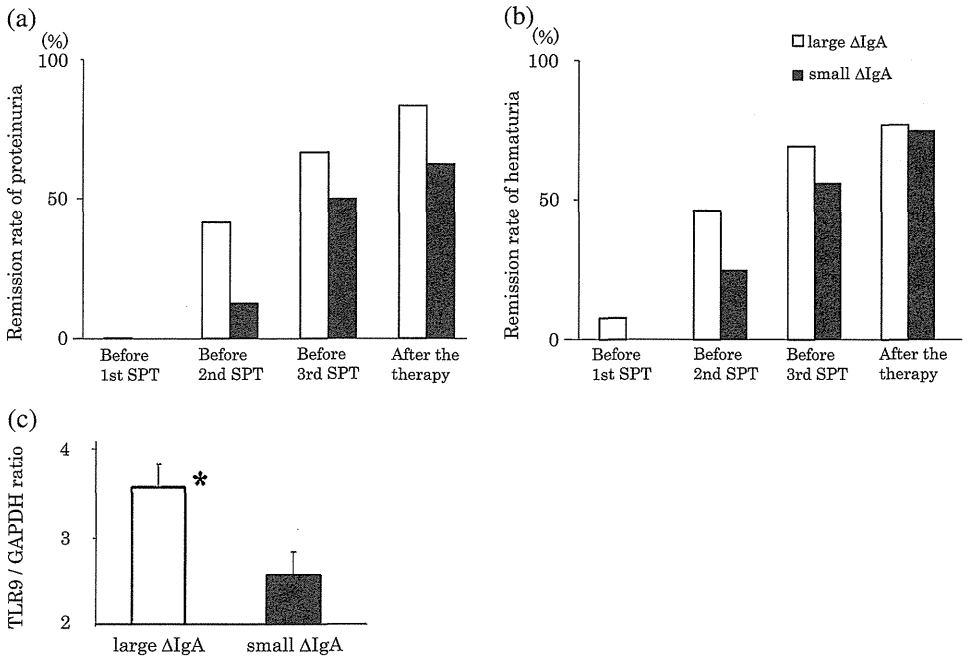

Fig. 2. (**a**, **b**) Clinical distinction between patients whose serum IgA decreased after tonsillectomy alone and patients whose serum IgA did not decrease. The IgAN patients were divided into two groups. The large ΔIgA group included patients whose serum IgA decreased more than the average (8.1%) following tonsillectomy alone (open bars). The remaining 16 patients were designated as the small ΔIgA group (filled bars). Comparison of the cumulative remission rates of proteinuria (a) and hematuria (b) showed the large ΔIgA group had higher remission rates than the small ΔIgA group. However, the remission rate of hematuria did not show the same tendency. (**c**) The expression levels of TLR9 in tonsils of the large ΔIgA group (open bars) was significantly higher than that of the small ΔIgA group (filled bars) ($P < 0.05$).

Table 5. Distribution of TLR9 SNP in large and small ΔIgA groups

	TT	CT/CC
Large ΔIgA	3	13
Small ΔIgA	4	8

further gated R1 using the pDC marker (anti-CD123 antibody) as R2 (Figure 3d). As shown in Figure 3e, certain parts of the R2 pDC population also expressed TLR9.

Discussion

A previous Japanese study on the clinical prognosis of IgAN patients with tonsillectomy concluded that tonsillectomy had a favorable effect on long-term renal survival [3]. Hotta *et al.* [4] reported that tonsillectomy combined with SPT had a significant impact on clinical remission, with histopathological improvements in IgAN patients after a median follow-up period of 75 months. The remission rate of hematuria associated with combination therapy reached ~80% regardless of the severity of the glomerular lesions. To avoid future aggravation of renal injury, these studies recommended this therapy for patients in the early stage of the disease before a 'point of no return' [17]. However, the indication for tonsillectomy in IgAN is controversial, even in Japan. Although tonsillectomy in certain patients can be an effective treatment, 7–10% of IgAN patients show spontaneous clinical remission [18]. Therefore, rationale and reasonable clinical markers are needed for indication of this therapy. Recent studies have shown that predictive factors for resistance to tonsillectomy with SPT are age at onset, severity of proteinuria and hematuria and pathological grade [19]. Although there is an ongoing randomized control trial concerning the effect of tonsillectomy on this disease, carried out by the Special Study Group on Progressive Glomerular Disease of the Ministry of Health, Labor and Welfare of Japan and the Japanese Society of Nephrology, the results are not yet available. Therefore, the present study aimed to evaluate the correlation between the efficacy of this therapy, tonsillar TLR9 expression and *TLR9* SNP in order to provide evidence for indications for tonsillectomy.

Our group recently reported a novel spontaneous IgAN-prone animal model. We found that human and murine IgAN are regulated, at least in part, by the same genes [20]. An association study using an IgAN-prone mouse showed that the progression of murine IgAN was linked to signaling molecules of TLR. We then examined the relationship between the TLRs mRNA expression levels in splenocytes and disease activity and found that the severity of glomerular injury in this model was clearly linked only to the degree of TLR9 expression in splenocytes [15]. In fact, intranasal immunization with CpG-ODN, an established ligand for TLR9, aggravated glomerular damage with an elevation in serum IgA levels. The present study demonstrates that some IgAN patients exhibit relatively high expression of tonsillar TLR9 mRNA (TLR9 high-group) and have an earlier more complete clinical remission than those with low expression (TLR9 low-group). These findings raise the possibility that TLR9 expression

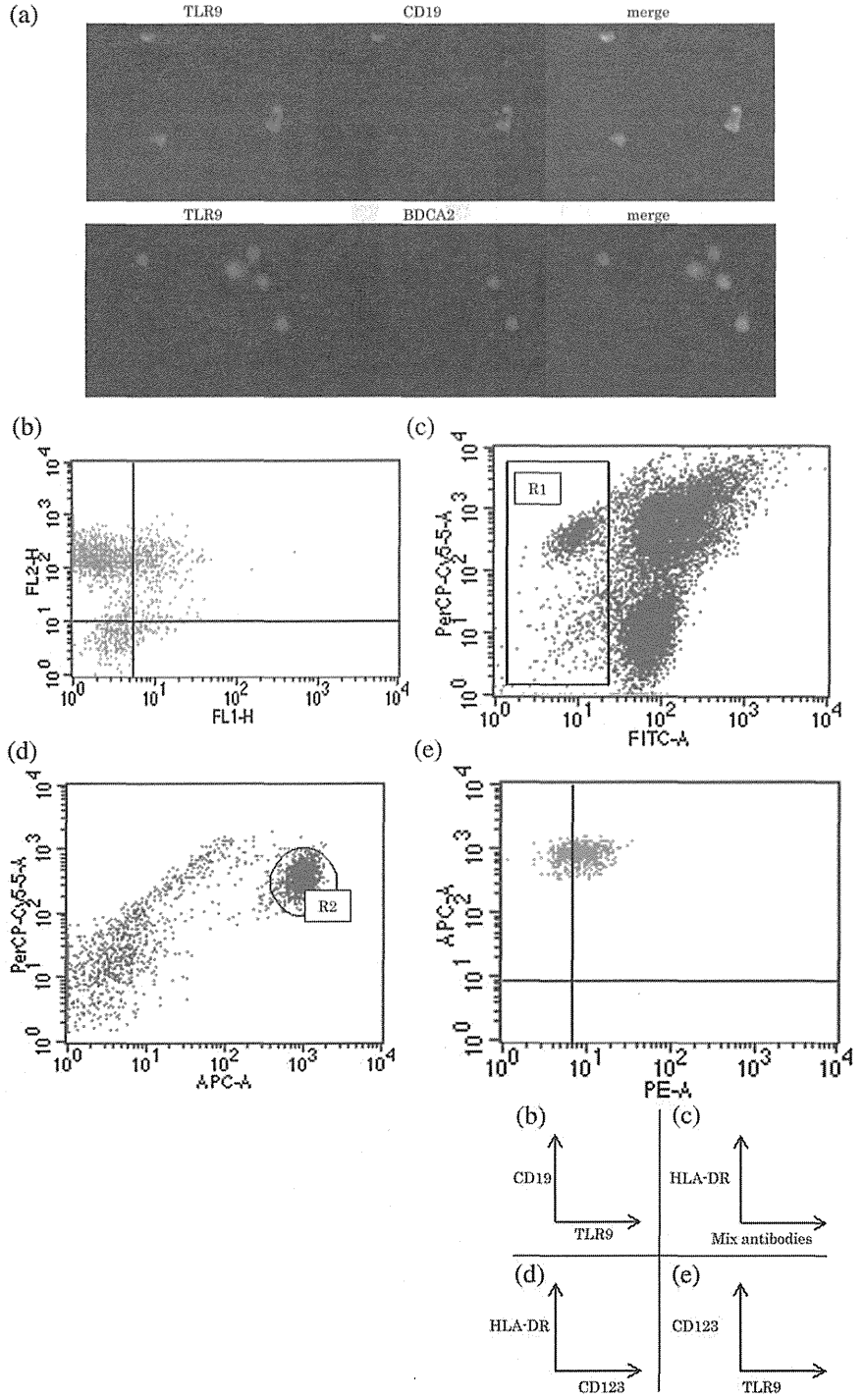

Fig. 3. TLR9 expressed on tonsillar B cells and pDC. (**a**) Fluorescence images and flow cytometric analysis confirmed TLR9 expression in B cells and plasmacytoid dendritic cells. (**b**) Certain parts of $CD19^+$ B cells expressed TLR9. (**c**) Lineage-negative (anti-human CD3, CD14, CD16, CD19, CD20 and CD56 antibodies) and HLA-DR-positive cells were gated as R1. (**d**) Further gating of R1 by the pDC marker (anti-CD123 antibody) as R2. (**e**) Certain parts of R2 (pDC population) also expressed TLR9.

is involved in the pathogenesis of not only murine but also human IgAN. Recent studies revealed that immunocompetent cells primed at mucosal sites may be recruited to other tissues by specific engagement of chemokines, chemokine receptors and adhesion molecules, suggesting that immunocompetent cells responsible for IgAN may also be primed in tonsils and disseminated to other systemic lymphoid tissues or bone marrow [21–23]. Therefore, surgical removal of tonsils may directly decrease the number of responsible cells and the chance of new priming in tonsils. Additional SPT may further eliminate the responsible disseminated cells. We consider that the mechanism

mediated by TLR9 may not be limited to the specific IgAN population. Although we also have an interest in the contribution of TLRs in kidneys and therefore examined this possibility in a previous study [15], we could not find a clear contribution, at least in murine IgAN. At present, we speculate that exogenous antigen may contribute mainly to the production of nephritogenic underglycosylated IgA (GdIgA) via TLR9 and subsequent immune complex formation with anti-glycan IgG but has no direct influence on renal resident cells in IgAN [21, 24]. Our previous study demonstrated that two genotypes of *TLR9* have a strong association with the progression of IgAN, further indicating the involvement of TLR9 in the pathogenesis of human IgAN [15]. We demonstrated that the CT/CC genotype in rs352139 and TT genotype in rs352140 could be risk factors for the progression of IgAN. As logistic regression analysis showed that *TLR9* SNP (rs352140) has a statistically strong association with the severity of pathological findings, we investigated *TLR9* SNP (rs352140) in IgAN patients in the present study. The histological prognostic criteria for the patients in the study tended to be similar to those reported previously [15]. The cumulative remission rate of proteinuria in patients with the CT/CC genotype of *TLR9* SNP (rs352140) was greater than in patients with the TT genotype. Moreover, in patients with the TT genotype, tonsillar inflammatory cytokine expression tended to be higher than in those with the CT/CC genotype. Although remission rates in patients with the TT genotype were lower than those in patients with the CT/CC genotype after the first SPT, cumulative remission rates of hematuria and proteinuria were almost the same on completion of this therapy. Therefore, early diagnosis and adequate treatment are important, particularly in the TT genotype patients, as their renal prognosis tends to become worse than that of the CT/CC genotype patients. Accordingly, *TLR9* SNP (rs352140) may be a good marker for aggressive treatment, including tonsillectomy with SPT.

The cumulative remission rate of proteinuria was higher in the large ΔIgA group than in the small ΔIgA group. Moreover, tonsillar TLR9 expression in the large ΔIgA group was significantly higher than in the small ΔIgA group. Snapshot evaluation of serum IgA level has limited clinical value for estimating disease activity. In fact, it is well known that only 30% of patients have high serum IgA levels. However, the findings of the present study suggest that the degree of reduction in serum IgA level after tonsillectomy may be related to the efficacy of this treatment and that tonsillar TLR9 may determine the serum IgA level in IgAN. GdIgA is thought to be involved in the pathogenesis of this disease [2, 25–27]. Moreover, IgA1 produced by tonsillar lymphocytes may be aberrantly glycosylated in IgAN patients [28, 29]. Therefore, tonsils may play an important role in the production of GdIgA1. On the other hand, the frequency of the CT/CC genotype was higher in the large ΔIgA group, which suggests that *TLR9* SNP (rs352140) may influence the amount of GdIgA production. However, as *TLR9* SNP (rs352140) is a non-coding lesion, further investigations are required.

In conclusion, the cells responsible for IgAN may exist in palatine tonsils and participate in the production of nephritogenic IgA mediated by the activity of TLR9. Therefore, tonsillar TLR9 expression level and *TLR9* SNP variation may influence the efficacy of tonsillectomy with SPT.

Acknowledgements. We are grateful to T Shibata and M Yamada for their excellent technical assistance. Parts of this study were supported by a Research Grant from the Study Group on IgAN in Japan and a Grant-in-Aid for Progressive Renal Disease Research, Research on intractable disease, from the Ministry of Health, Labor and Welfare of Japan.

References

1. Strippoli GF, Maione A, Schena FP *et al.* IgA nephropathy: a disease in search of a large-scale clinical trial to reliably inform practice. *Am J Kidney Dis* 2009; 53: 5–8
2. Barratt J, Feehally J. IgA nephropathy. *J Am Soc Nephrol* 2005; 16: 2088–2097
3. Xie Y, Nishi S, Ueno M *et al.* The efficacy of tonsillectomy on long-term renal survival in patients with IgA nephropathy. *Kidney Int* 2003; 63: 1861–1867
4. Hotta O, Miyazaki M, Furuta T *et al.* Tonsillectomy and steroid pulse therapy significantly impact on clinical remission in patients with IgA nephropathy. *Am J Kidney Dis* 2001; 38: 736–743
5. Sato M, Hotta O, Tomioka S *et al.* Cohort study of advanced IgA nephropathy: efficacy and limitations of corticosteroids with tonsillectomy. *Nephron Clin Pract* 2003; 93: 137–145
6. Komatsu H, Fujimoto S, Hara S *et al.* Effect of tonsillectomy plus steroid pulse therapy on clinical remission of IgA nephropathy: a controlled study. *Clin J Am Soc Nephrol* 2008; 3: 1301–1307
7. Masuda Y, Terazawa K, Kawakami S *et al.* Clinical and immunological study of IgA nephropathy before and after tonsillectomy. *Acta Otolaryngol Suppl* 1988; 454: 248–255
8. Tomioka S, Miyoshi K, Tabata K *et al.* Clinical study of chronic tonsillitis with IgA nephropathy treated by tonsillectomy. *Acta Otolaryngol Suppl* 1996; 523: 175–177
9. Bene MC, Faure G, Hurault de Ligny B *et al.* Immunoglobulin A nephropathy. Quantitative immunohistomorphometry of the tonsillar plasma cells evidences an inversion of the immunoglobulin A versus immunoglobulin G secreting cell balance. *J Clin Invest* 1983; 71: 1342–1347
10. Harper SJ, Feehally J. The pathogenic role of immunoglobulin A polymers in immunoglobulin A nephropathy. *Nephron* 1993; 3: 337–345
11. Kusakari C, Nose M, Takasaka T *et al.* Immunopathological features of palatine tonsil characteristic of IgA nephropathy: IgA1 localization in follicular dendritic cells. *Clin Exp Immunol* 1994; 95: 42–48
12. Akira S, Takeda K, Kaisho T. Toll-like receptors: critical proteins linking innate and acquired immunity. *Nat Immunol* 2001; 2: 675–680
13. Akira S, Takeda K. Toll-like receptor signalling. *Nat Rev Immunol* 2004; 4: 499–511
14. Takeuchi O, Akira S. Pattern recognition receptors and inflammation. *Cell* 2010; 140: 805–820
15. Suzuki H, Suzuki Y, Narita I *et al.* Toll-like receptor 9 affects severity of IgA nephropathy. *J Am Soc Nephrol* 2008; 19: 2384–2395
16. Tomino Y, Sakai H. Special study group (IgA nephropathy) on Progressive glomerular disease. Clinical guidelines for immunoglobulin A (IgA) nephropathy in japan, second version. *Clin Exp Nephrol* 2003; 7: 93–97
17. Hotta O. Use of corticosteroids, other immunosuppressive therapies, and tonsillectomy in the treatment of IgA nephropathy. *Semin Nephrol* 2004; 24: 244–255
18. Ibels LS, Gyory AZ, Caterson RJ *et al.* Recognition and management of IgA nephropathy. *Drugs* 1998; 55: 73–83
19. Miura N, Imai H, Kikuchi S *et al.* Tonsillectomy and steroid pulse (TSP) therapy for patients with IgA nephropathy: a nationwide survey of TSP therapy in Japan and an analysis of the predictive factors for resistance to TSP therapy. *Clin Exp Nephrol* 2009; 13: 460–466
20. Suzuki H, Suzuki Y, Yamanaka T *et al.* Genome-wide scan in a novel IgA nephropathy model identifies a susceptibility locus on murine

chromosome 10, in a region syntenic to human IGAN1 on chromosome 6q22-23. *J Am Soc Nephrol* 2005; 16: 1289–1299
21. Suzuki Y, Tomino Y. The mucosa-bone-marrow axis in IgA nephropathy. *Contrib Nephrol* 2007; 157: 70–79
22. Suzuki Y, Tomino Y. Potential immunopathogenic role of the mucosa-bone marrow axis in IgA nephropathy: insights from animal models. *Semin Nephrol* 2008; 28: 66–77
23. van den Wall Bake AW, Daha MR, Evers-Schouten J *et al.* Serum IgA and the production of IgA by peripheral blood and bone marrow lymphocytes in patients with primary IgA nephropathy: evidence for the bone marrow as the source of mesangial IgA. *Am J Kidney Dis* 1988; 5: 410–414
24. Suzuki Y, Suzuki H, Junichiro N *et al.* Pathological role of tonsillar B cells in IgA nephropathy. *Clin Dev Immunol* 2011, doi:10.1155/2011/639074
25. Novak J, Julian BA, Tomana M *et al.* Progress in molecular and genetic studies of IgA nephropathy. *J Clin Immunol* 2001; 5: 310–327
26. Mestecky J, Tomana M, Crowley-Nowick PA *et al.* Defective galactosylation and clearance of IgA1 molecules as a possible etiopathogenic factor in IgA nephropathy. *Contrib Nephrol* 1993; 104: 172–182
27. Coppo R, Amore A. Aberrant glycosylation in IgA nephropathy (IgAN). *Kidney Int* 2004; 5: 1544–1547
28. Horie A, Hiki Y, Odani H *et al.* IgA1 molecules produced by tonsillar lymphocytes are under-O-glycosylated in IgA nephropathy. *Am J Kidney Dis* 2003; 42: 486–496
29. Itoh A, Iwase H, Takatani T *et al.* Tonsillar IgA1 as a possible source of hypoglycosylated IgA1 in the serum of IgA nephropathy patients. *Nephrol Dial Transplant* 2003; 18: 1108–1114

Received for publication: 28.10.10; Accepted in revised form: 15.6.11

32. Cho KH, Kim HJ, Kamanna VS *et al.* Niacin improves renal lipid metabolism and slows progression in chronic kidney disease. *Biochim Biophys Acta* 2010; 1800: 6–15
33. Storch J, Thumser AE. The fatty acid transport function of fatty acid-binding proteins. *Biochim Biophys Acta* 2000; 1486: 28–44
34. Otvos JD, Collins D, Freedman DS. LDL and HDL particle subclasses predict coronary events and are changed favorably by gemfibrozil therapy in the Veterans Affairs HDL Intervention Trial (VA-HIT). *Circulation* 2006; 113: 1556–1563
35. Davidson MH, Armani A, McKenney JM *et al.* Safety considerations with fibrate therapy. *Am J Cardiol* 2007; 99: 3C–18C

Received for publication: 3.5.2012; Accepted in revised form: 22.6.2012

Nephrol Dial Transplant (2013) 28: 320–326
doi: 10.1093/ndt/gfs467
Advance Access publication 6 November 2012

Experimental evidence of cell dissemination playing a role in pathogenesis of IgA nephropathy in multiple lymphoid organs

Junichiro Nakata[1], Yusuke Suzuki[1], Hitoshi Suzuki[1,2], Daisuke Sato[1], Tatsuya Kano[1], Satoshi Horikoshi[1], Jan Novak[2] and Yasuhiko Tomino[1]

[1]Division of Nephrology, Department of Internal Medicine, Juntendo University Faculty of Medicine, Tokyo, Japan and [2]Department of Microbiology, University of Alabama at Birmingham, Birmingham, AL, USA

Correspondence and offprint requests to: Yasuhiko Tomino; E-mail: yasu@juntendo.ac.jp

Abstract

Background. Since the pathogenesis of immunoglobulin A (IgA) nephropathy (IgAN) remains unclear, the rationale for current IgAN therapies is still obscure. Recent studies have shown that galactose-deficient IgA1 (GdIgA1) plays a critical role in the pathogenesis of IgAN and can be a non-invasive IgAN biomarker, although the origin of the pathogenic cells producing GdIgA1 is unknown. We examined the cell types and localization of pathogenic cells in IgAN-prone mice.

Methods. We transplanted bone marrow (BM) or spleen cells with or without specific cell types from IgAN-prone mice, which have many features similar to human IgAN, to identify cell types responsible for the IgAN phenotype and to determine their localization.

Results. BM transplantation and whole spleen cell transfer from IgAN-prone mice reconstituted IgAN in normal and severe combined immunodeficiency mice. Depletion of $CD90^+$ spleen cells had no affect on reconstitution, whereas $CD19^+$ B cells from the spleen were sufficient to reconstitute IgAN in both recipients.

Conclusions. These results indicate that $CD19^+$ B cells, which can regulate nephritogenic IgA production in a T-cell-independent manner, are responsible for the disease and are disseminated in peripheral lymphoid organs.

Keywords: B cell; ddY mice; IgA nephropathy

Introduction

Clinical evidence from kidney transplantation studies indicates that the pathogenesis of immunoglobulin A (IgA) nephropathy (IgAN) is associated with an abnormality of the IgA immune system rather than with an abnormality intrinsic to the kidneys [1–4]. Episodic macroscopic hematuria coinciding with mucosal infections of the upper respiratory tract [5] or an abnormal response to mucosal vaccination in IgAN patients [6, 7] indicates that dysregulation of the mucosal immune system may play an important role in the pathogenesis of IgAN [8]. However, bone marrow (BM) and BM transplantation (BMT) studies in IgAN patients [9–12] suggest that nephritogenic IgA is overproduced at systemic immune sites such as BM. In the 1980s, van Es *et al.* hypothesized that a 'mucosa–BM axis' exists in IgAN in which there is continual trafficking of responsible cells in the IgA immune system between mucosal sites and BM [13, 14]. Clinical and experimental studies within the last decade have revealed the detailed mechanism by which lymphocytes traffic between mucosa and BM or lymphoid tissues. Although these findings support the original hypothesis, the cell types responsible for pathogenesis and their localizations remain unknown [15]. This is one of the reasons why no disease-specific therapy for IgAN exists.

Several studies have discussed whether IgAN is a stem-cell disease, since BMT with an IgAN donor reconstitutes IgAN in humans and mice [12, 16]. Because BM includes not only BM stem cells but also memory B cells [17], it should be carefully assessed whether the responsible cells are mature and are trafficked in the mucosa–BM axis. However, it is very difficult to experimentally access this in humans. We have recently established IgAN-prone mice, which show genetic and clinical features similar to those in human IgAN [18]. We found that IgAN can be

reconstituted in normal mice by BMT using IgAN-prone mice as donors [16]. In contrast, BMT from normal mice to IgAN-prone mice cures this disease, as observed in human IgAN [19]. Furthermore, mucosal activation of toll-like receptor-9 (TLR), a key molecule in innate and mucosal immunity, aggravates IgAN in these IgAN-prone mice [20], similar to that in humans [8, 20, 21]. These findings indicate that IgAN-prone mice may resemble human IgAN and thus can be a useful tool for assessing abnormalities in the mucosa–BM axis.

In this study, we analyzed the cell types and their localization using the IgAN-prone mice. Our findings provide new information on the pathogenesis of this disease.

Subjects and methods

Mice

We recently generated a new IgAN mouse model by inbreeding onset-ddY mice [6, 18]. The incidence of IgAN in the IgAN-prone mice was almost 100% [22, 23]. We used these IgAN-prone mice (approximately 20 weeks of age) as donors and 8- to 12-week-old female Balb/c and severe combined immunodeficiency (SCID) mice (C.B-17/Icr-scid/scidJcl, from CLEA Japan Inc., Tokyo, Japan) as recipients. Age-matched non-transferred female Balb/c and SCID mice were used as controls. The experimental protocol was approved by the Ethics Review Committee for Animal Experimentation of the Juntendo University Faculty of Medicine.

BMT And adoptive cell transfer in the mouse model

BM was harvested as described previously [16]. The spleen was enucleated under aseptic conditions. Spleen cell suspensions were prepared by compression with the handle of a syringe in RPMI-1640 medium containing 1% fetal calf serum (FCS) followed by passage through a 100-μm nylon mesh. Red blood cells were removed by incubation with ACK lysing buffer (0.15 M NH_4Cl, 1.0 mM $KHCO_3$ and 0.1 mM Na_2EDTA, pH 7.2) at room temperature for 5 min and washed in RPMI-1640 mediun containing 1% FCS [16]. $CD90^+$, $CD19^+$ and $CD138^+$ cells were depleted or isolated from BM and spleens of onset-ddY mice using CD90 (Thy1.2) MicroBeads, CD19 MicroBeads and the CD138 Plasma Cell Isolation Kit (MACS®, Milteny Biotec, Bergisch Gladbach, Germany) according to the manufacturer's instructions. Briefly, BM and spleen cells were resuspended at 1×10^7 cells/90 μl, and 10 μl of CD90 (Thy1.2) or CD19 MicroBeads was added to the cells at 4°C for 15 min. $CD90^+$ and $CD19^+$ cells were depleted or isolated by magnetic separation. To deplete $CD138^+$ cells, BM and spleen cells were resuspended at 1×10^8 cells/400 μl, and 100 μl of CD138 MicroBeads was added to cells at 4°C for 15 min. Then, the cells were depleted by magnetic separation. Purity of each preparation was assessed by flow cytometry.

Balb/c mice ($n = 6$) were irradiated, as described previously [16], while SCID mice ($n = 6$) were not. Next, $1–5 \times 10^8$ prepared cells were injected into the tail veins of mice on Day 0. The mice were housed under specific pathogen-free conditions. Urine samples were obtained every week and blood samples were obtained every 2 weeks after Day 28. Renal histology was analyzed at 4 and 8 weeks after transfer.

Methods of BMT and spleen cell transfer are shown in Figure 1.

Histological examination and serum IgA measurement and urinary albumin excretion in the mouse model

Renal specimens were fixed in 20% neutral phosphate-buffered formalin, embedded in paraffin and cut into 2-μm-thick sections. The slices were stained with hematoxylin and eosin, and periodic acid–Schiff. Snap-frozen 2-μm-thick renal sections were used for immunofluorescence with rhodamine-conjugated goat anti-mouse IgA (Santa Cruz Biotechnology, Inc., Santa Cruz, CA, USA). Immunofluorescence intensity was analyzed with ImageJ software (NIH, Bethesda, MD, USA), which calculated the sum of the intensity of each pixel. Serum IgG and IgA levels were measured using an ELISA kit (Mouse IgG ELISA Quantitation Kit or Mouse IgA ELISA Quantitation Kit, Bethyl Laboratories Inc., Montgomery, TX, USA). Urinary albumin was measured using an ELISA kit (Albuwell, Exocell, Philadelphia, PA, USA).

Statistical analysis

Correlations between different parameters were analyzed by the *t*-test. Analysis of variance was used to determine differences in characteristics among multiple groups. Data are expressed as mean ± SD or median values. $P < 0.05$ was considered significant. All statistical analyses were performed using the Windows version of StatView 5.0 software (Abacus Concepts Inc., Berkeley, CA, USA).

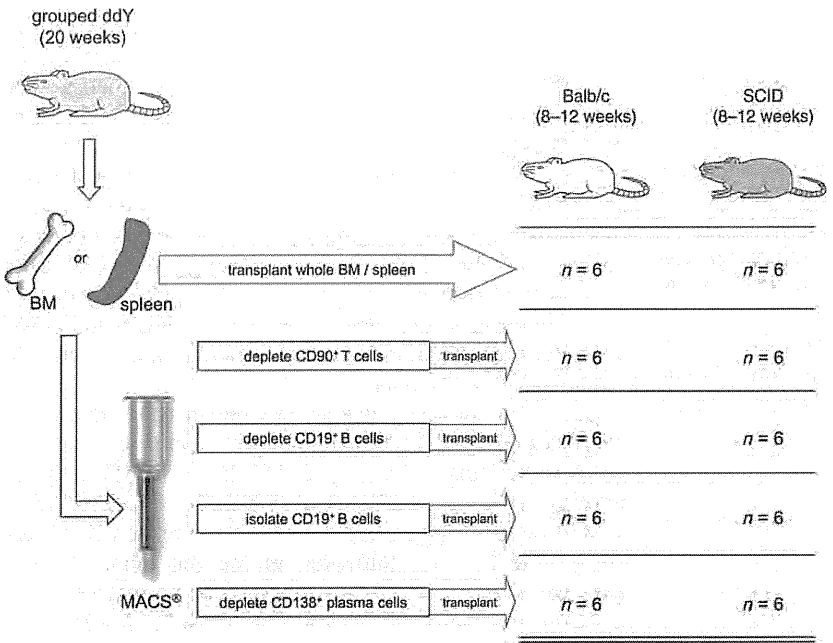

Fig. 1 . Method of BMT and spleen cell transfer.

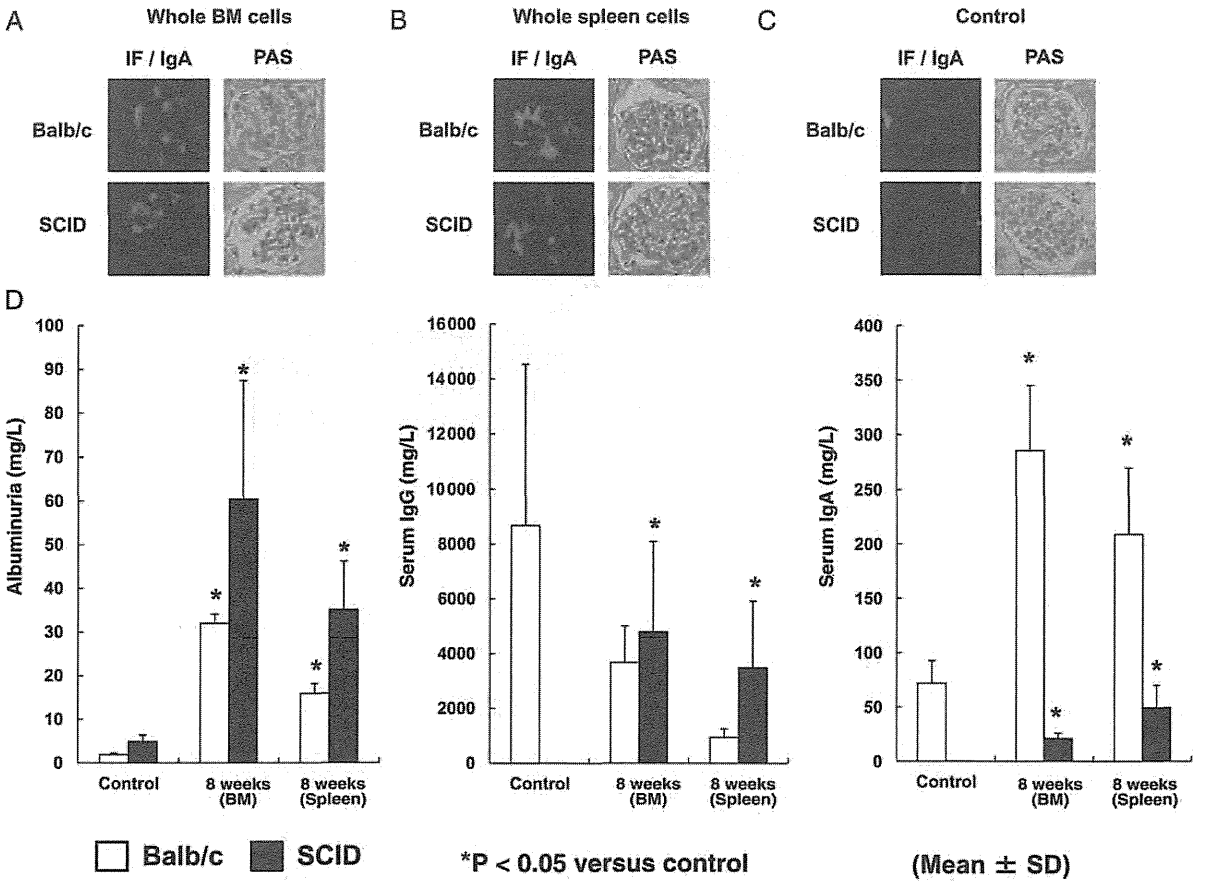

Fig. 2. (**A**) Complete BMT from IgAN-prone mice to Balb/c ($n=4$) and SCID ($n=4$) mice. Mesangial IgA deposition after complete BMT was observed even in SCID mice 8 weeks after transplantation. (**B**) Reconstitution of IgAN by whole spleen cell transfer from IgAN-prone mice to Balb/c and SCID mice. Mesangial IgA deposition with mesangial proliferation was observed in both Balb/c ($n=4$) and SCID ($n=4$) mice after the spleen cell transfer from IgAN-prone mice 8 weeks after transfer. (**C**) Age-matched non-transferred control Balb/c and SCID mice. Mesangial proliferation and mesangial IgA deposition were not observed in both mice. (**D**) Urinary albumin levels increased significantly together with a significant elevation in serum IgG and IgA levels 8 weeks after transfer of both BM and spleen.

Table 1. Intensity of immunofluorescence in Balb/c and SCID mice

	Balb/c	SCID
Control	0.55 ± 0.32	0.32 ± 0.18
Whole BM cells	21.66 ± 0.07	16.42 ± 3.37
BM without $CD90^+$ cells	10.74 ± 3.78	N.D
BM without $CD19^+$ cells	14.52 ± 0.04	N.D
BM without $CD138^+$ cells	12.23 ± 5.67	10.38 ± 4.46
Control	0.55 ± 0.32	0.32 ± 0.18
Whole spleen cells	16.04 ± 5.65	7.72 ± 2.09
CD90-depleted spleen cells	7.33 ± 3.00	6.89 ± 2.45
CD19-depleted spleen cells	0.07 ± 0.06	not successful
$CD19^+$ cells isolated from spleen	15.41 ± 10.84	15.30 ± 2.99
Spleen without CD138+ cells	12.27 ± 5.00	8.18 ± 4.48

Values are mean ± SD.

Results

Nephritogenic IgA-producing cells are derived from BM cells

Mouse IgAN with mesangial IgA deposition was reconstituted 8 weeks after complete BMT in both Balb/c and SCID mice (Figure 2A), as previously described [16]. In contrast, it was not shown in age-matched non-transferred control (Figure 2C). Urinary albumin levels increased significantly together with a significant elevation in serum IgG and IgA levels in SCID mice 8 weeks after transplantation (Figure 2D). Figure 3A shows the results of BMT with or without specific cells from ddY mice to Balb/c ($n=4$) or SCID ($n=4$) mice, which have no functional B or T lymphocytes. Quantitative analysis of fluorescence intensity is shown in Table 1. Glomerular IgA deposition was observed even in BM transplanted into Balb/c mice without $CD90^+$ pan T cells or without $CD19^+$ pan B cells 8 weeks after transplantation with increase in serum levels of IgA. Furthermore, BM without $CD138^+$ cells also reconstituted IgA deposition in both mouse strains 8 weeks after transplantation with increase of serum levels of IgA (Figure 3A and B).

Cells responsible for IgAN in mice are also in the spleen

To eliminate the potential effect of stem cells and examine whether mature pathogenic cells are disseminated to other lymphoid tissues, we performed spleen cell transfer from IgAN-prone mice. Figure 2B shows that whole

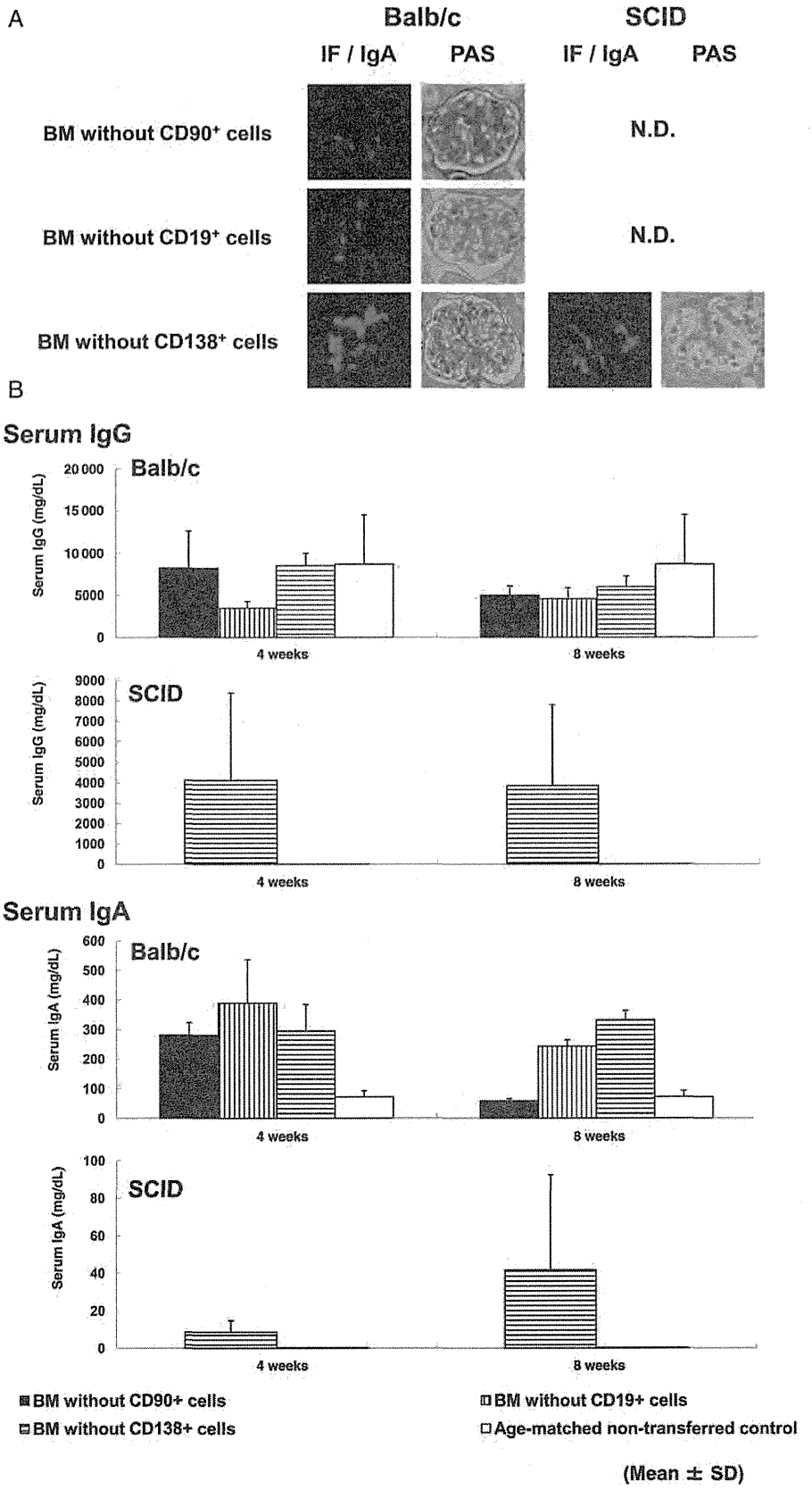

Fig. 3. (**A**) BMT with or without specific cell depletion from IgAN-prone mice to Balb/c ($n=4$) and SCID ($n=4$) mice. We observed mesangial IgA deposition after BMT without $CD90^+$ pan T cells, $CD19^+$ pan B cells or $CD138^+$ plasma cells (only in Balb/c: $n=4$) 8 weeks after transplantation. (N.D., not done) (**B**) Serum IgA levels increased after BMT, although IgG did not increase in Balb/c mice. In contrast, both IgG and IgA levels increased after BMT in SCID mice.

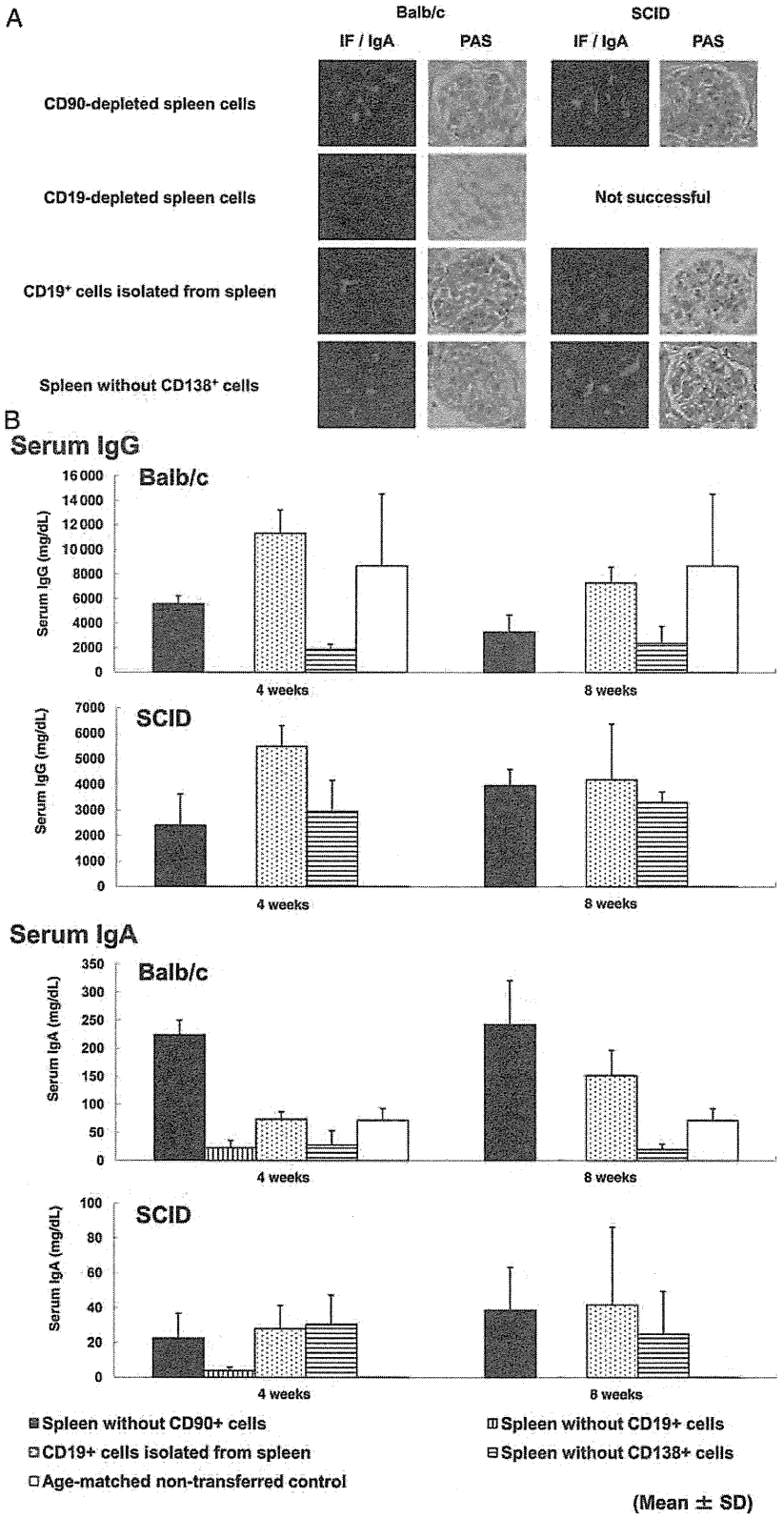

Fig. 4. Adoptive spleen cell transfer with or without specific cells from IgA nephropathy (IgAN)-prone mice to Balb/c ($n=4$) and SCID ($n=4$) mice. (**A**) Mesangial IgA deposition was observed in both mice 8 weeks after spleen cell transfer without $CD90^+$ pan T cells or with $CD19^+$ cells alone. In contrast, mesangial IgA deposition was not reconstituted after spleen cell transfer without $CD19^+$ cells into Balb/c mice 4 weeks after transfer, although transfer was not successful in SCID mice. Spleen cell transfer without $CD138^+$ cells reconstituted IgAN 8 weeks after transfer. (**B**) Serum IgG and IgA levels after adoptive transfer from IgAN-prone mice to Balb/c ($n=4$) or SCID ($n=4$) mice. Serum IgA levels increased in mice with IgA deposition, such as Balb/c mice with cell transfer without $CD90^+$ or $CD138^+$ cells and those undergoing single transfer of $CD19^+$ cells. Depletion of $CD90^+$ or $CD138^+$ cells and single transfer of $CD19^+$ cells also showed elevated serum IgA in levels in Balb/c and SCID mice.

spleen cell transfer reconstituted IgAN with glomerular IgA deposition and mesangial proliferation 8 weeks after transfer in both Balb/c ($n=4$) and SCID ($n=4$) mice. Serum IgA and urinary albumin levels 8 weeks after transfer in Balb/c ($n=4$) and SCID ($n=4$) were significantly higher than those in age-matched non-transferred normal control mice (Figure 2D). These findings revealed that cells responsible for IgAN in mice are also in the spleen.

$CD19^+$ Splenocytes induce mesangial IgA deposition independent of $CD90^+$ cells

Spleen cell transfer without $CD90^+$ pan T cells or $CD138^+$ plasma cells and transfer of $CD19^+$ cells alone resulted in the reconstitution of IgAN with mesangial IgA deposition in both mouse strains ($n=4$) 8 weeks after transfer (Figure 4A). Elevated serum IgA levels were observed even in the case of spleen cell transfer without $CD138^+$ cells in both strains ($n=4$, Figure 4B). In contrast, mesangial IgA deposition was not reconstituted 4 weeks after the spleen cell transfer without $CD19^+$ cells (Figure 4A). Furthermore, serum IgA levels were not elevated after the spleen cell transfer without $CD19^+$ cells (Figure 4B).

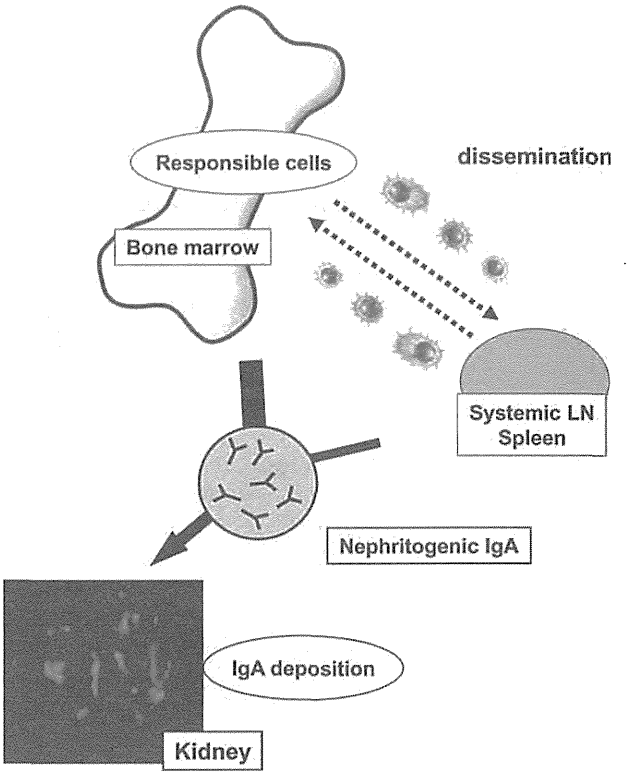

Fig. 5. A schematic representation of abnormalities in mucosa–BM axis.

Discussion

The present study provides important clues about cells responsible for IgAN development. IgAN-prone mice showed exacerbation of the disease together with an increase in serum IgA levels and glomerular IgA deposition via activation of mucosal TLR9 [20], suggesting that the responsible cells expressing TLR9 may be localized in the mucosa. Furthermore, we recently reported that mucosal activation of TLR9 on B and dendritic cells contributes to the progression of IgAN in mice following nasal cell-specific CpG-DNA challenges [24]. However, the present findings clearly showed that the responsible cells are localized not only in BM [16] but also in the spleen. Therefore, cells responsible for IgAN in mice may traffic in these organs as in human [25]. Adoptive transfer analyses showed that $CD19^+$ cells are necessary for developing IgAN in mice. CD19 is expressed on follicular dendritic and B cells. $CD19^+$ cells responsible for this disease may mainly be B cells, since $CD19^+$ cells transfer glomerular IgA deposition with an elevation in serum IgA levels in SCID mice lacking T and B cells.

CD19 is present in B cells from the earliest recognizable B-lineage cells during development to B-cell blasts but is lost after plasma cells mature [26]. In contrast, CD138 is a well-known cell-surface marker for plasma cells [27]. In this study, BMT without $CD138^+$ cells and spleen cell transfer without $CD138^+$ cells induce glomerular IgA deposition or glomerular lesions in both Balb/c and SCID mice. Pre-B or immature B cells in BM of mice expressed CD138. Cells lost CD138 expression after emigrating from BM, but re-expressed it during final maturation to plasma cells in peripheral lymphoid tissues or the spleen. Therefore, the responsible cells for reconstitution of IgA deposition may be $CD19^+$ B cells, but not mature $CD138^+$ plasma cells, from IgAN-prone mice. Meanwhile, it was reported that B-cell progenitors might be in the spleen or peritoneal cavity, suggesting that those might circulate generally. Furthermore, those might generate Ig-secreting cells on some conditions [28]. Therefore, circulating B cell progenitors might sense the environment during its circulation in peripheral lymphoid organs and generate nephritogenic IgA secreting cells.

Reconstitution of IgAN by spleen cell transfer depleted of $CD90^+$ pan T cells in both mouse strains and transfer of $CD19^+$ cells in SCID mice indicates that the responsible B cells produced nephritogenic IgA in a T-cell-independent manner. Our recent experimental study using alymphoplasia (aly/aly) mice [29] further supports this hypothesis (Figure 5). Aly/aly mice have no secondary lymphoid tissues or germinal center (GC) [30]. However, BMT from our IgAN-prone mice also reconstituted glomerular IgA deposition and glomerular lesions in aly/aly-recipient mice [29], suggesting that a somatic hypermutation in GC may not be required for nephritogenic IgA production at least in IgAN in mice. Therefore, nephritogenic IgA-producing B cells may mature in GC- and T-independent manners. If the responsible cells include memory B cells, they may be T-independent natural memory cells, but not T-dependent switched memory B cells or long-lived IgA plasma cells [31, 32]. Moreover, human IgAN is not generally associated with a marked cellular infiltration into glomeruli, suggesting that the development of glomerular injury after IgA deposition is mediated predominantly through IgA-induced

activation of resident mesangial cells and local complement activation. As glomerular lesions become more severe, the number of mononuclear cells, but not T cells, increases both in the mesangium and Bowman's space [32]. This result may provide some clues for the clinical facts that T-cell infiltration in human IgAN are less than the other glomerulonephritis [33].

Our experimental studies with IgAN-prone mice, which have genetic and pathological background similar to human IgAN [16, 18, 22, 23], demonstrated that cells responsible for the pathogenesis of IgAN may be $CD19^+$ B cells, and these cells disseminated not only to mucosa but also to other lymphoid tissues such as BM and the spleen. Furthermore, our preliminary data of clinical treatment response by tonsillectomy with steroid pulse therapy indicate that cells producing aberrant IgA may be disseminated to systemic organs, although they mainly localize in mucosa, particularly in the tonsils. Although it is necessary to establish a method to objectively evaluate the extent of dissemination in the systemic organs and consider the indication for each therapy including immunosuppressants targeting the disseminated cells, the current findings provide important clues not only for pathogenesis but also treatment strategies of IgAN.

Acknowledgements. The authors thank T. Shibata, M. Yamada and all members of the laboratory for technical support and helpful discussions.

Funding. A part of this study was supported by research funds from Grant-in-Aids for Progressive Renal Disease Research, Research on Intractable Disease, from the Ministry of Health, Labor and Welfare of Japan, a grant from Strategic Japanese (JST)-Swiss (ETHZ) Cooperative Scientific Program and a grant from the Study Group on IgA Nephropathy in Japan.

Conflict of interest statement. None declared.

References

1. Floege J, Burg M, Kleige V. Recurrent of IgA nephropathy after kidney transplantation: not a benign condition. *Nephrol Dial Transplant* 1998; 13: 1933–1935
2. Floege J. Recurrent IgA nephropathy after renal transplantation. *Semin Nephrol* 2004; 24: 287–291
3. Cuevas X, Lloveras J, Mir M *et al.* Disappearance of mesangial IgA deposits from the kidney of two donors after transplantation. *Transplant Proc* 1987; 19: 2208–2209
4. Sanfilippo F, Croker BP, Bollinger RR. Fate of four cadaveric donor renal allografts with mesangial IgA deposits. *Transplantation* 1982; 33: 370–376
5. Emancipator SN. Immunoregulatory factors in the pathogenesis of IgA nephropathy. *Kidney Int* 1990; 38: 1216–1229
6. de Fijter JW, Eijgenraam JW, Braam CA *et al.* Deficient IgA1 immune response to nasal cholera toxin subunit B in primary IgA nephropathy. *Kidney Int* 1996; 50: 952–961
7. Roodnat JI, de Fijter JW, van Kooten C *et al.* Decreased IgA1 response after primary oral immunization with live typhoid vaccine in primary IgA nephropathy. *Nephrol Dial Transplant* 1999; 14: 353–359
8. Suzuki Y, Tomino Y. Potential immunopathogenic role of the mucosa-bone marrow axis in IgA nephropathy: insights from animal model. *Semin Nephrol* 2008; 28: 66–77
9. Feehally J. Immune mechanisms in glomerular IgA deposition. *Nephrol Dial Transplant* 1988; 3: 361–378
10. van den Wall Bake AW, Beyer WE, Evers-Schouten JH *et al.* Humoral immune response to influenza vaccination in patients with primary immunoglobulin A nephropathy. An analysis of isotype distribution and size of the influenza-specific antibodies. *J Clin Invest* 1989; 84: 1070–1075
11. Harper SJ, Allen AC, Pringle JH *et al.* Increased dimeric IgA producing B cells in the bone marrow in IgA nephropathy determined by in situ hybridisation for J chain mRNA. *J Clin Pathol* 1996; 49: 38–42
12. Imasawa T, Nagasawa R, Utsunomiya Y *et al.* Bone marrow transplantation attenuates murine IgA nephropathy: role of a stem cell disorder. *Kidney Int* 1999; 56: 1809–1817
13. van den Wall Bake AW, Daha MR, van Es LA. Immunopathogenetic aspects of IgA nephropathy. *Nephrologie* 1989; 10: 141–145
14. van Es LA, van den Wall Bake AW, Stad RK *et al.* Enigmas in the pathogenesis of IgA nephropathy. *Contrib Nephrol* 1995; 111: 169–176
15. Kunkel EJ, Butcher EC. Plasma-cell homing. *Nat Rev Immunol* 2003; 3: 822–829
16. Suzuki H, Suzuki Y, Aizawa M *et al.* Th1 polarization in murine IgA nephropathy directed by bone marrow-derived cells. *Kidney Int* 2007; 72: 319–327
17. Tokoyoda K, Hauser AE, Nakayama T *et al.* Organization of immunological memory by bone marrow stroma. *Nat Rev Immunol* 2010; 10: 193–200
18. Suzuki H, Suzuki Y, Yamanaka T *et al.* Genome-wide scan in a novel IgA nephropathy model identifies a susceptibility locus on murine chromosome 10, in a region syntenic to human IGAN1 on chromosome 6q22–23. *J Am Soc Nephrol* 2005; 16: 1289–1299
19. Iwata Y, Wada T, Uchiyama A *et al.* Remission of IgA nephropathy after allogeneic peripheral blood stem cell transplantation followed by immunosuppression for acute lymphocytic leukemia. *Intern Med* 2006; 45: 1291–1295
20. Suzuki H, Suzuki Y, Narita I *et al.* Toll-like receptor 9 affects severity of IgA nephropathy. *J Am Soc Nephrol* 2008; 19: 2384–2395
21. Sato D, Suzuki Y, Kano T *et al.* Tonsillar TLR9 expression and efficacy of tonsillectomy with steroid pulse therapy in IgA nephropathy patients. *Nephrol Dial Transplant* 2012; 27: 1090–1097
22. Zuo N, Suzuki Y, Sugaya T *et al.* Protective effects of tubular liver-type fatty acid-binding protein against glomerular damage in murine IgA nephropathy. *Nephrol Dial Transplant* 2011; 26: 2127–2137
23. Okazaki K, Suzuki Y, Otsuji M *et al.* Development of a model of early-onset IgA nephropathy. *J Am Soc Nephrol* 2012; 23: 1364–1374
24. Kajiyama T, Suzuki Y, Kihara M *et al.* Different pathological roles of toll-like receptor 9 on mucosal B cells and dendritic cells in murine IgA nephropathy. *Clin Dev Immunol* 2011; 2011: 819646
25. Suzuki H, Moldoveanu Z, Hall S *et al.* IgA1-secreting cell lines from patients with IgA nephropathy produce aberrantly glycosylated IgA1. *J Clin Invest* 2008; 118: 629–639
26. Carter RH, Myers R. Germinal center structure and function: lessons from CD19. *Semin Immunol* 2008; 20: 43–48
27. Sanderson RD, Lalor P, Bernfield M. B lymphocytes express and lose syndecan at specific stages of differentiation. *Cell Regul* 1989; 1: 27–35
28. Ghosn EE, Sadate-Ngatchou P, Yang Y *et al.* Distinct progenitors for B-1 and B-2 cells are present in adult mouse spleen. *Proc Natl Acad Sci USA* 2011; 108: 2879–2884
29. Aizawa M, Suzuki Y, Suzuki H *et al.* Roles of bone marrow, mucosa and lymphoid tissues in pathogenesis of murine IgA nephropathy. *Contrib Nephrol* 2007; 157: 164–168
30. Shinkura R, Matsuda F, Sakiyama T *et al.* Defects of somatic hypermutation and class switching in alymphoplasia (aly) mutant mice. *Int Immunol* 1996; 8: 1067–1075
31. Weill JC, Weller S, Reynaud CA. Human marginal zone B cells. *Annu Rev Immunol* 2009; 27: 267–285
32. Pillai S, Cariappa A. The follicular versus marginal zone B lymphocyte cell fate decision. *Nat Rev Immunol* 2009; 9: 767–777
33. Barratt J, Smith AC, Molyneux K *et al.* Immunopathogenesis of IgAN. *Semin Immunopathol* 2007; 29: 427–443

Received for publication: 5.4.2012; Accepted in revised form: 13.8.2012

The Kinetics of Glomerular Deposition of Nephritogenic IgA

Kenji Yamaji[1], Yusuke Suzuki[1], Hitoshi Suzuki[1], Kenji Satake[1], Satoshi Horikoshi[1], Jan Novak[2], Yasuhiko Tomino[1]*

1 Division of Nephrology, Department of Internal Medicine, Juntendo University School of Medicine, Tokyo, Japan, **2** Department of Microbiology, University of Alabama at Birmingham, Birmingham, Alabama, United States of America

Abstract

Whether IgA nephropathy is attributable to mesangial IgA is unclear as there is no correlation between intensity of deposits and extent of glomerular injury and no clear mechanism explaining how these mesangial deposits induce hematuria and subsequent proteinuria. This hinders the development of a specific therapy. Thus, precise events during deposition still remain clinical challenge to clarify. Since no study assessed induction of IgA nephropathy by nephritogenic IgA, we analyzed sequential events involving nephritogenic IgA from IgA nephropathy-prone mice by real-time imaging systems. Immunofluorescence and electron microscopy showed that serum IgA from susceptible mice had strong affinity to mesangial, subepithelial, and subendothelial lesions, with effacement/actin aggregation in podocytes and arcade formation in endothelial cells. The deposits disappeared 24-h after single IgA injection. The data were supported by a fluorescence molecular tomography system and real-time and 3D in vivo imaging. In vivo imaging showed that IgA from the susceptible mice began depositing along the glomerular capillary from 1 min and accumulated until 2-h on the first stick in a focal and segmental manner. The findings indicate that glomerular IgA depositions in IgAN may be expressed under the balance between deposition and clearance. Since nephritogenic IgA showed mesangial as well as focal and segmental deposition along the capillary with acute cellular activation, all glomerular cellular elements are a plausible target for injury such as hematuria.

Citation: Yamaji K, Suzuki Y, Suzuki H, Satake K, Horikoshi S, et al. (2014) The Kinetics of Glomerular Deposition of Nephritogenic IgA. PLoS ONE 9(11): e113005. doi:10.1371/journal.pone.0113005

Editor: Johan van der Vlag, Radboud university medical center, Netherlands

Received July 15, 2014; **Accepted** October 17, 2014; **Published** November 19, 2014

Data Availability: The authors confirm that all data underlying the findings are fully available without restriction. All relevant data are within the paper and its Supporting Information files.

Funding: A part of this study was supported by research funds from Grant-in-Aids for Progressive Renal Disease Research, Research on intractable disease, from the Ministry of Health, Labor and Welfare of Japan, a grant from Strategic Japanese (JST)-Swiss (ETHZ) Cooperative Scientific Program and a grant from the Study Group on IgA Nephropathy in Japan. The funders had no role in study design, data collection and analysis, decision to publish, or preparation of the manuscript.

Competing Interests: The authors have declared that no competing interests exist.

* Email: yasu@juntendo.ac.jp

Introduction

Immunohistological analysis is the crux of the diagnosis of IgA nephropathy (IgAN) for which dominant or co-dominant mesangial deposition of IgA is essential. Significant number of patients is reported to have elevated levels of circulating IgA immune complexes (IC), presumably due to aberrantly glycosylated IgA and endogenous antiglycan antibodies [1–3]. Thus, primary IgAN is an IC-mediated glomerulonephritis that is immunohistologically defined by the presence of glomerular IgA deposits accompanied by various histopathologic lesions. However, whether IgAN is attributable to mesangial IgA or IgA IC deposition remains unclear. One mystery is the lack of correlation between the intensity of deposits and the extent of glomerular injury; in addition, a long-standing question remains whether these mesangial IgA deposits directly induce hematuria [3–6]. To the best of our knowledge, no definitive study provides a comprehensive answer to these questions.

In contrast, we also know patients who exhibit minor clinical symptoms, such as very low levels of hematuria and proteinuria but have massive glomerular IgA depositions, suggesting that not all IgA immune deposits possess equivalent pathogenic potential. These conflicting clinical findings make it difficult to identify the true therapeutic target of this disease, thereby hindering the development of a specific therapy [7], [8]. Thus, despite almost half a century of clinical and basic research, the immunologic processes that induce and perpetuate glomerular IgA deposition and the detailed mechanism underlying deposition events remain unknown. IgAN may represent multiple diseases with abnormal urinary findings, sharing common pathogenic markers, such as mesangial IgA immune deposits, and having unknown mechanisms whereby damage is propagated in a discontinuous pattern [5]. The deposition of circulating IgA/IgA-containing IC may be the most likely mechanism; an understanding of the detailed sequential events in pathogenesis is the key to developing a successful therapy [2], [3], [9], [10].

We recently established a strain of spontaneous IgAN-prone gddY mice in which the disease phenotype and genetic regulation largely overlap with human IgAN [11–13]. Although abnormal glycosylation of *O*-linked glycans in the hinge region of human IgA1 is linked to human IgAN [2], [3], it has long been believed that *O*-glycans are absent in the hinge region of murine IgA. However, our recent paper [12] revealed that more severe disease

in gddY mice occurs in those with an IgA allotype that has less sugar content in the hinge region. Thus, modification of carbohydrate structures may change the conformational or biochemical properties of murine IgA, thereby altering the nephritogenicity or formation of IgA-IC, as seen in human IgAN [2]. Moreover, aberrantly glycosylated IgA may induce macromolecular IgA complex formation, leading to the complement activation and subsequent progression to IgAN [14], as seen in human IgAN [2], [9]. Furthermore, serum levels of IgA-IgG IC correlate with the severity of renal damage in IgAN-prone mice [15]. Our recent reports demonstrate that cells responsible for producing nephritogenic IgA are disseminated in the mucosa-bone marrow axis [15–18] and are regulated by the innate immune system [19–21], as seen in human IgAN [13], [19], [22], [23]. Accordingly, experimental, immunological, and histopathological findings in this susceptible strain seem to recapitulate the clinical features of human IgAN [11–13]. Details of the sequence of events in glomerular deposition of nephritogenic IgA from IgAN have not been described in the literature. In the present study, we use nephritogenic IgA from this susceptible mouse strain to examine this sequence of events using a real-time imaging system. Sequential analysis of IgA-induced IgAN may provide clues to the pathogenesis of this disease and strategies for its treatment.

Materials and Methods

Mice

The gddY mice were established by the selective mating of early-onset ddY mice for more than 20 generations and have a 100 % incidence of severe disease, even at a young age [11–16]. The gddY mice were maintained on a regular chow (MF; Oriental Yeast, Tokyo, Japan) and water *ad libitum* in a specific pathogen-free (SPF) room at the animal facility of Juntendo University, Tokyo, Japan.

Same-age female Balb/c (Balb/c) mice were used as controls. Female Balb/c AJcl-nu/nu (nude) mice were used for the injection of serum or IgA from the gddY mice with early-stage disease and from the Balb/c mice. Balb/c and nude mice were purchased from CLEA Japan Inc., Tokyo, Japan. The experimental protocol of the present study was approved by the Ethics Review Committee for Animal Experimentation of Juntendo University Faculty of Medicine.

The serum single-injection model

Serum samples were obtained from gddY mice aged between 20 and 25 weeks who showed severe renal injury with glomerular IgA deposits. Serum from age-matched healthy Balb/c mice was also collected as the control serum. Serum levels of IgA were measured using a single radioimmunodiffusion assay (SRL, Tokyo, Japan). The obtained serum samples, including 2 mg IgA of gddY or Balb/c mice (300 μL, diluted with saline) were injected once into the tail vein of nude mice aged between 10 and 12 weeks. The nude mice were euthanized either 2 or 24 h after the injection of serum. Kidneys were collected from the nude mice after perfusion with normal saline solution. The serum samples and kidneys were stored at −80°C until use. Renal histological analysis was performed using electron and confocal microscopy.

Snap-frozen 3-μm-thick renal sections were used for immunofluorescence with a fluorescein isothiocyanate-conjugated goat antimouse IgA antibody (BD Biosciences, San Diego, CA, USA; Pharmingen, San Diego, CA, USA). For electron microscopy, the renal specimens were fixed in 2 % glutaraldehyde, washed in phosphate buffer, and postfixed in 1 % osmic acid. The specimens were washed, dehydrated, and embedded in Epon 812. The ultrathin sections were contrasted with uranyl acetate and lead citrate and then examined under an electron microscope (Hitachi 7100, Tokyo, Japan).

Purification of IgA

Serum samples were obtained from the gddY and Balb/c mice aged between 20 and 25 weeks. Each serum sample was incubated with a rat antimouse IgA antibody with CNBr Sepharose overnight at 4°C. After washing with phosphate-buffered saline (PBS), IgA was eluted with 0.1 M glycine (pH 2.5) using a fraction collector. Molecular size of purified IgA obtained from ddY and Balb/c mice were analyzed by Western blot analysis. The purified IgA samples were used for fluorescence molecular tomography and confocal laser microscopy analyses.

Kinetic studies using a fluorescence molecular tomography system

These studies were conducted on female nude mice (n = 3). The purified IgA samples obtained from gddY or Balb/c mice were labeled with Vivo Tag-S 750 (VisEn Medical Inc. Woburn, MA, USA). Purified IgA samples were dissolved at 2 mg/mL in PBS, and 0.5 mL of the solution was alkalized with 50 μL of 1 M sodium bicarbonate solution. The mixture was incubated with Vivo Tag-S 750 for 1 h at room temperature, with stirring. The labeled IgA was purified using resin column chromatography. Fluorescein-labeled IgA (0.5 mg/mL) was dissolved in 200 μL PBS and injected into nude mice aged between 10 and 12 weeks. After 2, 4, and 24 h, IgA signals were measured using a fluorescence molecular tomography system (VisEn Medical Inc. Woburn, MA, USA).

Kinetic studies by confocal laser microscopy

Kinetic studies by confocal laser microscopy were performed in female nude mice (n = 3). Purified IgA obtained from gddY or Balb/c mice was labeled using an Alexa Fluor 633 protein labeling kit (Molecular probes, Inc., Eugene, OR, USA). Purified IgA samples were dissolved at 2 mg/mL in PBS, and 0.5 mL of the solution was alkalized with 50 μL of a 1 M sodium bicarbonate solution. The mixture was incubated with Alexa Fluor 633 dye at room temperature for 1 h, with stirring. The labeled IgA was purified using resin column chromatography. Before analysis, the nude mice were anesthetized with sodium pentobarbital. An incision of approximately 10 mm was made on the lower back, and a kidney was removed using small forceps. The surface of the lower pole of the kidney was sliced and placed on a microscope stage. Dextran (500 kDa) is not filtered and is a good marker for blood vessel wall integrity. First, fluorescein-labeled 500-kDa dextran (Sigma–Aldrich Inc., St. Louis, MO, USA) was injected into nude mice to confirm the staining of glomeruli. Following this, fluorescein-labeled IgA (0.5 mg/mL) was dissolved in 200 μL PBS and injected into mice. After 1 and 120 min, the kinetics of labeled IgA in glomeruli were analyzed using confocal laser microscopy (ZEISS, LSM 510 META, Germany). Single or time-series images of glomeruli were recorded in fluorescence mode.

The procedure of BMT

The procedure for murine BMT was previously described in detail [15–18]. In brief, BMC were harvested from the tibia, femur, and humerus of control Balb/c mice at 8–10 weeks of age under sterile conditions. Red blood cells were removed from the collected BMC. Grouped ddY mice develop glomerular lesions with mesangial IgA deposits within 6–8 weeks of age [11], [12]. Young and old gddY mice aged 8 and 20 weeks who were at the early stage of the disease were used as recipients. Following this,

10^7 BMCs were injected into the tail vein of irradiated recipient mice (n = 3) at 700 rad. The recipient mice were housed under SPF conditions. Young and old gddY transplant recipients were euthanized 12 weeks after BMT. IgA deposits were assessed by immunofluorescence and electron microscopy, and urinary protein was measured by immunoassay (DCA 2000 system; Siemens Healthcare Diagnostics, Tokyo, Japan).

Results

A single injection of serum from gddY mice, but not from Balb/c mice, induced glomerular IgA deposition with an activation of glomerular podocytes and endothelial cells

We first tested whether a serum from gddY mice induced glomerular IgA deposition in nude mice. Serum from Balb/c mice was used as a control. Renal tissue was obtained from nude mice euthanized 2 and 24 h after a single injection of the serum. Serum from gddY mice, but not Balb/c mice, induced mesangial IgA deposition 2 h after the injection (Fig. 1a). The electron-dense deposits in the paramesangial areas were confirmed using electron microscopy (Fig. 1b). After 2 h, in some glomeruli of the mice injected with the gddY mouse serum, electron-dense deposits were detectable in subepithelial and subendothelial lesions, with effacement and actin aggregation in the podocytes and arcade formation in some endothelial cells. This data is indicative of the activation of those cells (Fig. 1c). Such morphological changes were not found with injections of Balb/c IgA (serum to be precise; data not shown). In this single-injection model, mesangial IgA deposition and electron-dense deposits almost disappeared after 24 h (Fig. 1a and b, right panels).

IgA from gddY mice showed high affinity for kidney tissue

We next labeled serum IgA from gddY mice and control Balb/c mice with Vivo Tag-S 750 and analyzed the *in vivo* kinetics of IgA using a fluorescence molecular tomography system after a single injection in nude mice. After the injection of IgA from gddY or Balb/c mice, fluorescence signals in the kidneys, liver, and bladder were evaluated after 10 min and 2, 4, and 24 h. There was no difference in the signals in the liver and bladder between the mouse groups that received labeled IgA from either gddY or Balb/c mice (Fig. 2, middle and lower panels). Two hours after injection, IgA signals were detected in the kidneys of both groups by molecular tomography (Fig. 2 upper panels). However, the renal signals in mice injected with IgA from gddY mice increased, with a peak at 4 h after the injection, whereas renal signals in controls were weak and gradually decreased.

IgA from gddY mice is deposited along the glomerular capillary wall in a focal and segmental manner

To further clarify the sequential manner of the deposition process, we injected Alexa Fluor 633 protein-labeled IgA (red) from gddY and Balb/c mice and fluorescein-labeled 500-kDa Dextran (green) to visualize the glomerular capillary in the nude mice. We then analyzed the glomerular capillaries using confocal laser microscopy from 1 min to 2 h after the single injection (Fig. 3). Yellow images indicate IgA deposition along the glomerular capillaries. This *in vivo* real-time/3D imaging (Fig. 3a and supporting information in video and 3D images) confirmed the data from previous immunofluorescent analysis, electron microscopy, and tomography, in that IgA from gddY has a higher affinity for the glomerulus than that from Balb/c mice. Nevertheless, this gddY-derived IgA was deposited along the glomerular capillary in a focal and segmental manner. This *in vivo* imaging with a focus on the glomerular capillary showed initial deposition after only 1 min (Fig. 3b). IgA accumulated on top of these first aggregates or microdeposits (Fig. 3c); however, this accumulation was not diffuse. Two hours after the injection, the amount of labeled IgA in the glomerular capillary gradually decreased in both groups of mice. Nonetheless, a clear accumulation of IgA in glomerular mesangial areas was found in the *in vivo* imaging with a focus on mesangial areas after 2 h in the group injected with IgA from gddY mice, but not in that from Balb/c mice. Molecular forms of both IgA purified from ddY and Balb/c mice were analyzed by Western blotting under non-reducing condition. IgA purified from ddY mice serum was predominantly polymeric with a small peak of dimeric IgA. IgA purified from Balb/c mice was monomeric and dimeric dominant (data not shown).

Glomerular IgA deposits in old gddY mice remained after bone marrow transplantation (BMT) despite improved proteinuria

To clear IgAN in gddY mice [14], [15], we transplanted bone marrow cells (BMC) from Balb/c (healthy) mice into gddY mice. We confirmed the disappearance of proteinuria in both young and old recipients 12 weeks after BMT [albuminuria before vs. after BMT (μg/day): young recipients, 121.3±21.2 vs. 26.3±6.7; old recipients, 198.0±23.0 vs. 30.3±12.9]. However, fluorescence analysis still detected glomerular IgA deposition in old but not young gddY recipients (Fig. 4 left panels). Electron microscopy detected dense paramesangial deposits in the old recipients; however, these dense deposits showed fibrous and lattice structures.

Discussion

The primary abnormal clinical manifestation of IgAN in patients is recurring bouts of hematuria with or without associated proteinuria [3], [4]. In the complex web of potential mechanisms implicated in the pathogenesis of IgAN, mesangial IgA deposits remain a *sine qua non*. This notion may lead us to believe that mesangial IgA deposition directly induces hematuria. However, there are no studies proving a direct relationship between the amount mesangial IgA immune deposits and the extent of glomerular injury leading to hematuria. Our earlier comprehensive observations emphasized the variable characteristics of the IgA/IgA IC, particularly the nature of antigens and the molecular form of IgA, as major determinants of glomerular injury [10]. Several physical characteristics, including size, lattice composition, electric charge, and glycosylation, may also influence the probability of deposition in the glomerular mesangium [2], [3], [9], [10], [24–31]. Sequential events were analyzed in the experiments with artificially modified IgA or IgA IC. Even these observations failed to provide a sufficient explanation for the mechanisms leading to hematuria in IgAN. This may be partly due to the absence of experiments with IgA preparations that have been confirmed to induce a chronic progression of IgAN with mesangial cell proliferation and matrix expansion. Thus, this appears to be the first study to assess the kinetics of glomerular deposition of nephritogenic IgA in IgAN [11–16].

The present analysis using tomography showed a similar time course of liver signals peaking at 2 h in both the groups of mice, indicating that most of the injected IgA from the gddY and control mice was trapped in the liver in a similar fashion. The parts of injected IgA from both the groups of mice passed through into the bladder in a similar manner. Nevertheless, renal signals were conspicuously stronger in the group injected with IgA from gddY

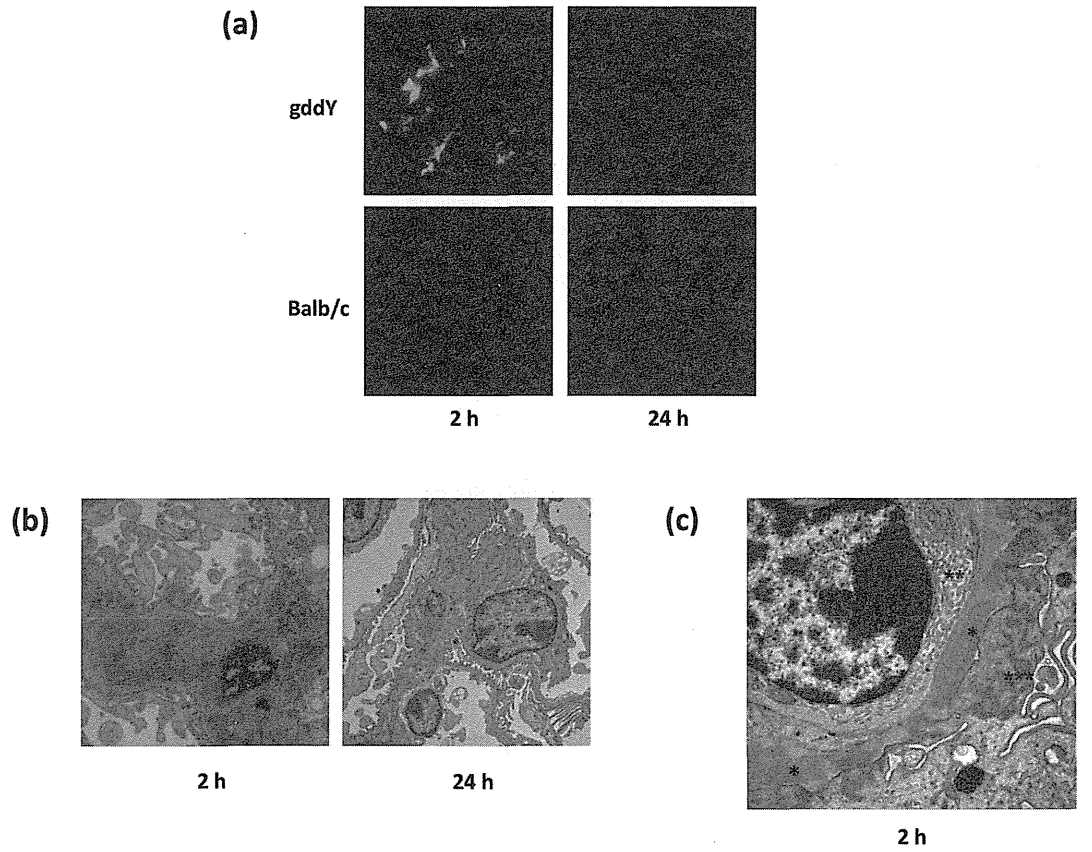

Figure 1. A single injection of serum from gddY mice induced glomerular IgA deposition with activation of glomerular podocytes and endothelial cells. (a) Glomerular IgA deposits were found at 2 h in mice injected with serum from gddY mice but not from Balb/c mice. These fluorescent signals disappeared after 24 h in this single-injection model. (b) These deposits and clearance were confirmed using electron microscopy. Electron-dense deposits were mainly detected in paramesangial lesions. (c) Some glomeruli showed subendothelial and subepithelial deposits (*) with arcade formation in glomerular endothelial cells (**) and effacement and actin aggregation in podocytes (***) 2 h after the injection.
doi:10.1371/journal.pone.0113005.g001

mice than in those injected with IgA from healthy mice. This finding indicates that some clones of IgA in gddY mice have a strong affinity for kidney tissues and may be nephritogenic. Our recent studies have shown that IgA in gddY mice is polymeric and that it has a high capacity for activating complement cascades, including the lectin pathway [14]. The renal prognosis of this susceptible model is likely to be dependent on the content of carbohydrates in the hinge region of IgA [12]. Recent research has also suggested that aberrant N-glycan glycosylation may be involved in the pathogenesis of IgAN in mice [32], [33]. These findings suggest that aberrant modifications of serum IgA carbohydrate side chains are involved in the development of IgAN, not only in humans but also in mice, regardless of whether the carbohydrates are O-glycans or N-glycans [2], [3], [13]. Recent studies have revealed that aberrantly glycosylated IgA1 (GdIgA1) plays a nephritogenic role in this disease [1–3], [9], [34]. The serum level of GdIgA1 is associated with the disease activity of IgAN [35]. On the other hand, anomalous glycosylation of IgA is a key determinant of glomerular affinity [31]. Thus, the high glomerular affinity found in the present study may be partly due to the basic molecular nature of IgA, presumably with aberrant glycosylation.

The disappearance of the glomerular deposits in this single-injection model is one of most important findings of the present study. This finding indicates that a continuous clearance mechanism of IgA deposition may be at work in the glomerulus. Thus, glomerular IgA deposits in IgAN may be explained as an imbalance between deposition and clearance. Although most IgAN patients have undoubtedly had glomerulonephritis for years before a renal biopsy, it seems that a certain percentage of IgAN patients may go through a clinical period just after the onset, when neither IgA nor C3 is detectable in the renal biopsy but when there are histological lesions and aberrant urinary test results [7], [8]. Thus, our results indicate that the intensity of staining for IgA in the kidney may wax or wane based on the balance in the glomeruli or mesangium.

Increasing evidences suggest that mucosal type polymeric IgA1 is produced in BM of IgAN patients [36]. Furthermore, BMT in patients with leukemia and IgAN resulted in the cure of not only leukemia but also IgAN [37]. Therefore, cross talk between the mucosa and BM is suspected in the pathogenesis of IgAN [13], [38], [39]. We previously showed that murine IgAN can be reconstituted via BMT from ddY mice to healthy mice [15–18], [40]. We also showed that early-stage IgAN in ddY mice can be cured by removing glomerular IgA via BMT from healthy mice [15], [16]. However, glomerular IgA deposits in the present BMT model from healthy mice to ddY mice disappeared in young but not old ddY recipients; proteinuria in both young and old recipients was alleviated by BMT. This finding suggests that incompletely cleared IgA deposition in the disease course of gddY mice may change in conformation or biochemical properties as a result of their organization or fibrosis with mesangial matrix